Chapter 1
Techniques for Large-Scale Multiunit Recording

Hendrik W. Steenland and Bruce L. McNaughton

Abstract Single and multineuron extracellular electrophysiology has proven to be one of the most effective techniques to explore the behavior of neurons in freely behaving animals since the 1950s. Electrode technology has evolved over the past 60+ years, with improvements in electrode profiles, configurations, biocompatibility, and driving mechanisms leading to substantial gains in the isolation of single neuron activity and increases in the possible number of simultaneously recorded neurons. Moreover, combining electrode recording and nanotechnology with pharmacological and optogenetic manipulations are expected to bring about a new age for precise recording and manipulation of neurons. In this chapter we review the technical developments of extracellular electrophysiology in freely behaving animals, with special emphasis on the development of microelectrode technology.

Keywords Microelectrode • Hyperdrive • Electrophysiology • Extracellular • Freely behaving

Extracellular Recording

Deriving the Extracellular Action Potential

The extracellular action potential is derived from currents flowing across the resistive extracellular medium between charged locations on the cell surface. The voltage drop between these locations is a consequence of ion conductance, most notably voltage-sensitive sodium and potassium channels. The primary advantage of extracellular recording is that neural activity can be recorded without puncturing the cell membrane, thus making recordings more stable over long time periods. Also, multiple neurons can be often detected on the same extracellular probe, capturing more accurately the population dynamics. One disadvantage is that the extracellular

H.W. Steenland, Ph.D. • B.L. McNaughton, Ph.D. (✉)
Department of Neuroscience, University of Lethbridge,
440l University Drive W, Lethbridge, AB TlK 3M4, Canada
e-mail: hendrik.steenland@uleth.ca; bruce.mcnaughton@uleth.Ca

M. Tatsuno (ed.), *Analysis and Modeling of Coordinated Multi-neuronal Activity*, Springer Series in Computational Neuroscience 12,
DOI 10.1007/978-1-4939-1969-7_1

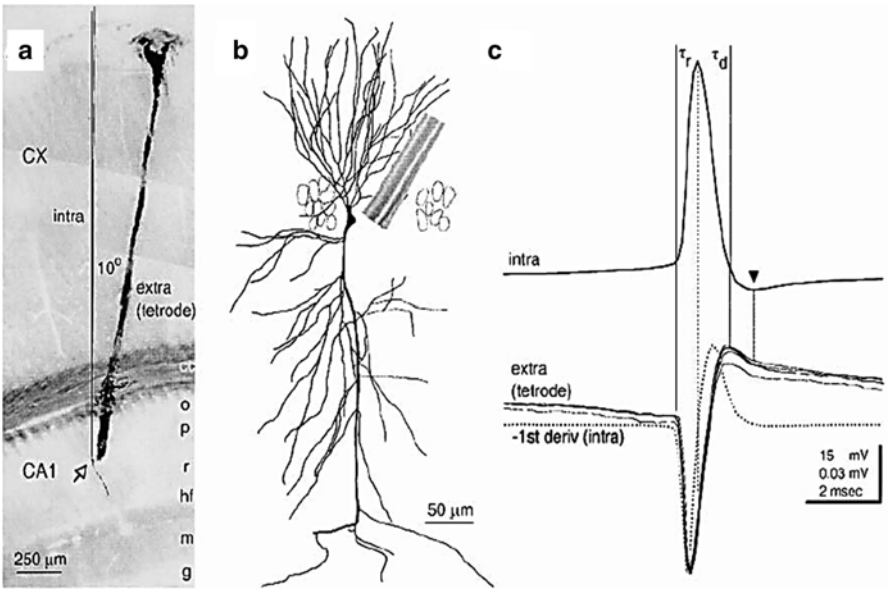

Fig. 1.1 Deriving the extracellular spike waveform. (**a**) Histological representation of an intracellular electrode and an angled extracellular tetrode recording (marked by angled blood stain) from the same cell in the CA1 pyramidal layer (*open triangle*) of an anesthetized rat. Intracellular electrode is drawn on the figure as a *vertical line*. (**b**) Camera lucida reconstruction of the intracellular recorded neuron under study. Tetrode is drawn adjacent to neuron soma. (**c**) Comparison of intracellular (*top*) and extracellular waveforms (*bottom dark line*). Note taking the negative first derivative of the intracellular waveform approximates the early components of the extracellular waveform. (**a**, **b**, and **c**) Reprinted with permission from Henze DA, Borhegyi Z, Csicsvari J, Mamiya A, Harris KD, Buzsaki G. Intracellular features predicted by extracellular recordings in the hippocampus in vivo. J Neurophysiol. 2000;84(1):390–400

potentials tend to be in the range of ~100 µV, two orders of magnitude less than transmembrane potentials. This poses challenges due to both intrinsic noise of the recording system, typically in the low microvolt range [1], and "far-field" noise due to signals from other neurons. The latter can be partially overcome with specialized methods to isolate the signals from individual neurons including careful positioning of fine-tipped electrodes close to individual cells, "triangulation" of neuron signals by recording simultaneously at several nearby points in space [2], and application of algorithms and statistics to separate neurons based on their waveform features [3, 4].

The relationship of the extracellular potential waveform to transmembrane potentials (i.e., membrane currents) has practical implications for sorting multiunit activity and identifying neuronal classes (e.g., bursting cells). To this end, pioneering electrophysiologists carried out simultaneous intracellular and extracellular recording from the same cell [5]. More recently, Henze et al. [6] conducted simultaneous intra- and extracellular recording of hippocampal CA1 neurons in an anesthetized rat preparation. Figure 1.1a, b illustrates a sharp glass electrode penetrating a pyramidal CA1 cell for intracellular recording with an adjacent tetrode [7–9] to

record the extracellular spike discharge. As indicated in earlier studies [10, 11], it was found that the negative first derivative of the intracellular signal closely approximates the detected extracellular waveform (Fig. 1.1c). Note that the negative going phase of the extracellular signal is a consequence of inward current near the soma due to altered gNa^+ (sodium conductance). It can also be appreciated that the time course of the first negative peak of the extracellular waveform closely matched the negative first derivative of the intracellular signal corresponding to depolarization. In addition, it was shown that changes in action potential amplitudes due to cell bursting could be observed at the extracellular level.

Equivalent Electrical Circuit for Recording Extracellular Potentials

We can use electrical circuits ("equivalent circuits") (Fig. 1.2) to represent the extracellular recording configuration. The first consideration is the recording configuration. Typical high-quality in vivo electrophysiology requires a minimum of three connections to the animal body. The first connection is the ground lead which is used as a return line for the headstage power. Additionally, when the final termination point of this ground is connected to a Faraday cage, which encapsulates a preparation, 60 Hz line noise can be dramatically reduced. The remaining two electrodes are the recording and the reference electrodes. The recording electrode can be positioned near cells of interest to monitor changes in extracellular potential. The reference electrode is often placed in a region of low cell density such as a fiber bundle, minimizing signals from other neurons but hopefully recording the same "far-field" noise as the active electrode. This noise can include 60 Hz mains external noise or internally generated noise such as heartbeats or masseter chewing artifacts. In conjunction with a differential amplifier, the reference electrode is used to subtract common mode signals (i.e., noise) from the signals of interest (i.e., local action potentials). Accordingly, an ideal reference electrode would record the same undesired signals as the active electrode [12, 13].

To record from neurons in freely behaving animals, signals are usually buffered with a unity gain (1×) headstage to increase the electrical current while maintaining the signal voltage (hence, 1× gain). This increase in signal current reduces the impact of interfering currents generated in the tether leads. These interfering currents are generated as a consequence of electromagnetic fields (e.g., from AC power sources) and cable flexion, while the signal current is carried from the headstage to the amplifier. In addition, the headstage requires very high input impedance (Z value) to prevent it from dramatically influencing the signal being sampled [14] and should be located as close to the signal source as possible. Since electrodes are not protected on the input side of the headstage from noise pickup, they should be protected from mechanical vibration.

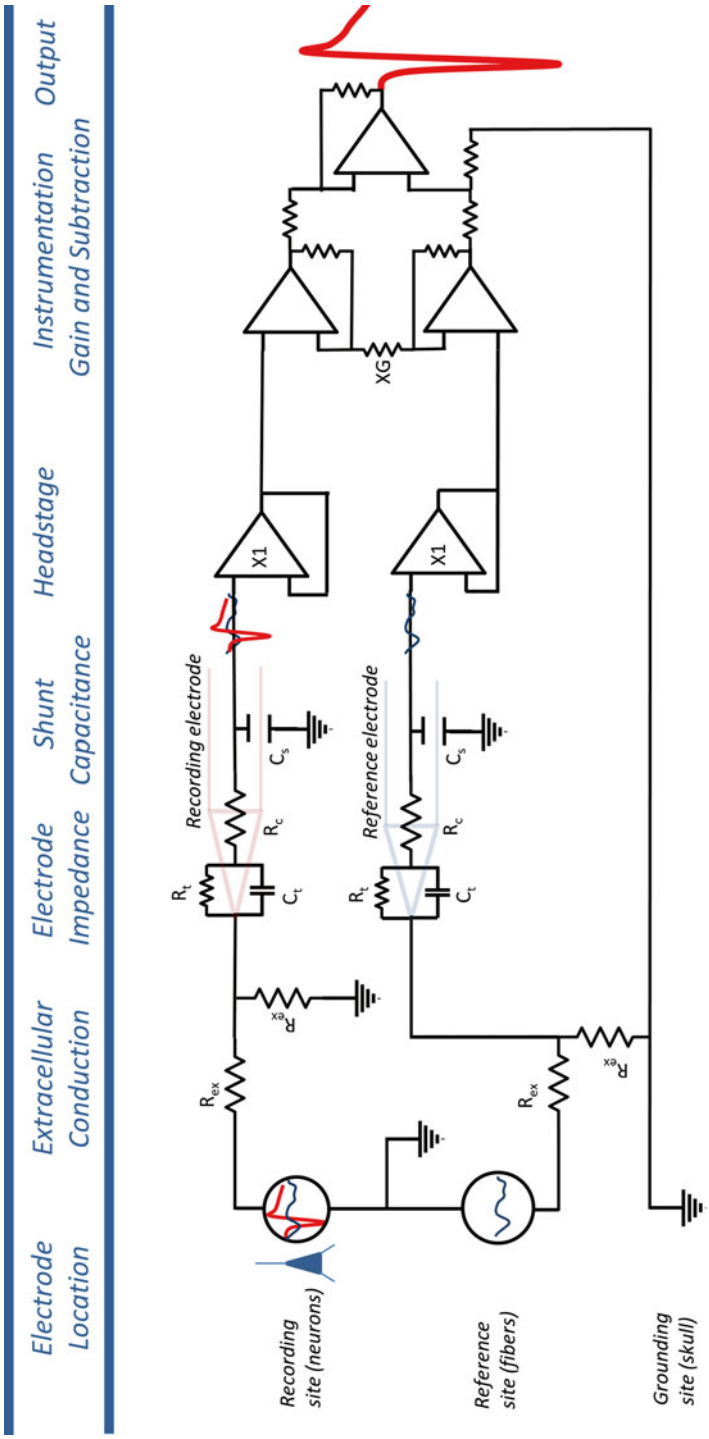

Fig. 1.2 Equivalent circuit for extracellular spike recording. Generally, a minimum of three contacts are made to the subject, including a recording, reference, and ground electrodes. Changes in extracellular ion concentrations are transmitted across the resistance (R_{ex}) of the extracellular space to the recording and reference electrode tips. This signal must interface with the electrode tip through its impedance (resistance of tip R_t and capacitance of tip C_t). Once the charge has passed the electrode tip, some of the signal is lost due to dissipation across the capacitance of the electrode insulation. The resistance of the electrode material is denoted by "Rc". The signal travels to the headstage, where the voltage is held constant (X1) but the current is amplified and therefore protected (or buffered) from environmental interference. The signal is then sent to a differential (instrumentation) amplifier that subtracts out the common components between the two signals (presumably background noise) to purify the signal of interest. This amplifier also adds a degree of gain (XG) so that the signal range can match that of the analog to digital conversion (not shown)

The Extracellular Recording Volume

Extracellular currents are generated whenever there are voltage differences between two points on a neuron, such as when there is a spike generated at the soma or when excitatory synapses are activated on a dendrite. These points of different potential are commonly referred to as current sources (local positivity) and sinks (local negativity). Because the extracellular fluids are a passive, resistive medium, these currents result in extracellular potential fields relative to a remote neutral (ground) point. For elongated, asymmetric cells, like typical neurons, these potential fields resemble (approximately) a simple dipole field, because the currents flow in loops around the cell (Fig. 1.3a). Thus, the sign of the potential at a particular point in time at a given point along the neuron depends on whether current has depolarized the cell at that spatial location, leaving a net negative charge outside the cell. Moreover, the magnitude of the dipole at a particular point depends on the voltage associated with the local current density relative to a reference point. The current decreases proportionately to the inverse square of the distance from the dipole [15, 16], and in general, the greater the distance between the points of different potential (dipole separation), the further the current spreads. Thus, at a given distance, larger fields tend to be generated by cells with longer dendrites. For further discussion on the field potentials and current source density, see Leung [17].

How much does the extracellular signal decrease with distance from its source? Rosenthal [18] estimated the extracellular voltage-distance relationship to be represented by the decay function 100 mV/(x)μm, where x is the distance from the neuron. At 250 μm distance from a cell body, one would expect a 400 μV signal. By contrast, voltage estimates based on data from the hippocampus, while following the same decay trend, are much lower. For example, Henze et al. [6] found that recordings from CA1 pyramidal cells, within a 100 μm radius, tended to be 60 μV or less with tetrodes, much less than that estimated by Rosenthal. Suffice it to say that there is a strong decline in extracellular amplitudes as the recording electrode is moved away from the neuron or source.

How many neurons can an extracellular electrode detect? The potential number of neurons in a specific volume of tissue can be compared to the actual number of neurons recorded. Henze et al. [6] argued that since the density of neurons in CA1 hippocampus is 300,000 cells/mm^3 [5], if the recording volume was a cylinder of 50 μm radius and height of 60 μm, then potentially 141 neurons should be recorded on one electrode (Fig. 1.4). For the motor cortex, assuming a density of 30,000/mm^3 [19] for the cortical cells, one would expect a comparable volume of 14 recordable neurons. Henze et al. [6] argued that their discrepancy with the actual number of neurons might be due to the fact that a large percentage of cells may not have sufficiently high spontaneous activity. Another possibility is that damage to tissue could reduce the viable recording population either by killing some neurons or by changing the pathways of current flow. Finally the possibility exists that a tortuous (non-isotropic) path taken by the extracellular signal to reach the electrode impacts the number of recordable cells.

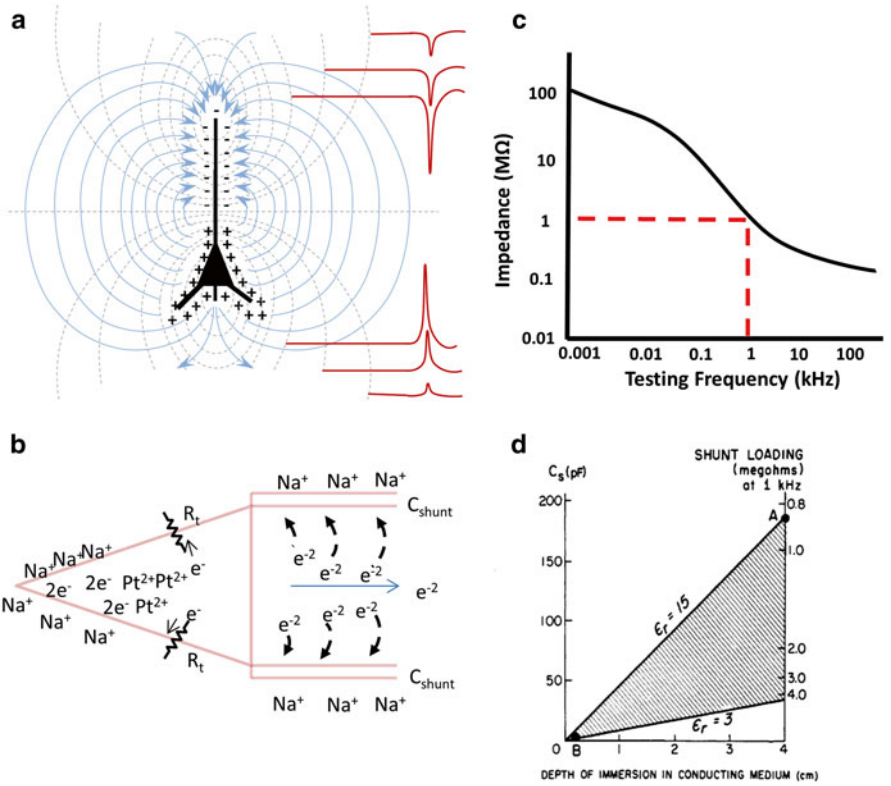

Fig. 1.3 Electrode-electrolyte interface. (**a**) Dipole representation of pyramidal neuron. Current is represented by *solid lines* traveling from source (+) to sink (−) in the extracellular space. Equipotential regions are represented by *dashed lines. Red lines* represent theoretical action potentials recorded at different distances from the source or sink. Signal strength decays with distance from the source and sink regions. (**b**) Theoretical illustration of the electrode-electrolyte interface. When the electrode is interfaced with the extracellular medium a bilayer forms between the electrode (e^- electrons) and electrolyte (Na^+). This forms the capacitive component of the electrode impedance and is responsible for the charge transfer in polarizable electrodes (note, other electrolytes have been excluded for simplicity). The resistive (R_t) component of the electrode impedance can also permit charge transfer. Shunt capacitance (C_{shunt}) acts to dissipate the charge transfer to the recording equipment if the insulation is insufficient. (**c**) Electrode impedance of a metal electrode as a function of frequency. Note high-impedance electrodes (>100 k**Ω** at 1 kHz) are optimized for high-frequency signal detection. *Red dotted lines* indicate typical impedances of the electrode before electroplating measured with a BAK impedance meter at 1 kHz. With kind permission from Springer Science + Business Media: Medical and Biological Engineering, Glass-coated platinum-plated tungsten microelectrodes, 1972, 662–72, Merrill EG, Ainsworth A. (**d**) Estimated shunt capacitance (C_{shunt}) for two different electrode insulations (varnish, dielectric $\epsilon_r = 3$, and solder glass, dielectric $\epsilon_r = 15$) in two different solutions (saline and mineral oil respectively) at different emersion depths in their respective mediums. The right-hand ordinate is a plot of the shunt impedance to ground or the impedance to signal loss. Electrode with a low dielectric insulation and insulated by mineral oil has the least signal loss. Thus according to this plot, shunt capacitance may only become a problem if the immersion depth in the brain is deep (e.g., >4 cm) and insulation is not optimized. © 1968 IEEE. Reprinted, with permission, from Robinson DA. Electrical Properties of Metal Microelectrodes. Proceedings of the Institute of Electrical and Electronics Engineers. 1968;56(6):1065–71

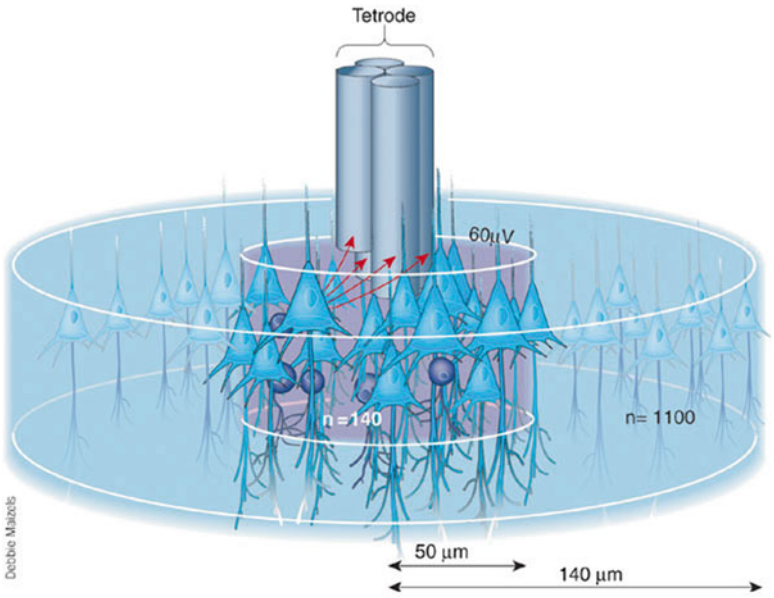

Fig. 1.4 Extracellular recording volume. Estimated number of potentially recordable CA1 neurons in the vicinity of a tetrode. One hundred and forty neurons of greater than 60 **μ**V should potentially be recorded within a 50 **μ**m radius (*purple volume*) of the tetrode. Reprinted with permission from Macmillan Publishers Ltd: Nature Neuroscience, Buzsaki G, Large-scale recording of neuronal ensembles, 7(5):446–51, copyright 2004 [98]

The extracellular field is composed of contributions from "dipoles" from numerous neurons, depending on local neural density and firing rates. This creates the complication that many neurons may be of the same type and may therefore generate similar action potential waveforms. An additional complication arises when spikes from two or more nearby neurons overlap in time; their extracellular potential waveforms summate, making the isolation of individual waveforms essentially impossible. Therefore, the traditional basis for extracellular "single" unit recording has been to select neurons by placing a fine-tipped electrode close enough to a particular neuron in a field of neurons. Because of this proximity the individual voltage contribution of that particular neuron will be greater than those in the far field (a benefit of the dipole inverse square function); however, such selectivity is difficult and renders the signal much more sensitive to slight movements of the electrode relative to the neuron (a negative consequence of the inverse square function, since the rate of change of signal with distance is larger closer to the origin).

Electrode-Electrolyte Bilayer

When electrodes are inserted into electrolyte or extracellular solution, cations and anions are thought to form an electrode-electrolyte interface termed a bilayer [20, 21] (Fig. 1.3b). Electronically this bilayer can be modeled as a combination of

resistance and capacitance components, which is collectively known as impedance (inductive component of impedance is not discussed). Impedance is a measure of the opposition to an alternating current (AC) flow. This concept is especially important, as the electrical currents in and around cells can also be considered alternating currents changing over timescales of about a millisecond. If this bilayer is formed, how then does current pass into the electrode to be picked up by the headstage? As we will see, whether or not an electrode is easily oxidized will determine whether neurons are recorded via capacitive discharge or direct conductance through the resistive surface of the electrode tip.

Polarized Versus Nonpolarized Electrodes

Theoretically two types of electrodes exist, those that are polarizable and those that resist polarization [20]. Ideally a perfectly polarizable electrode displaces current through loading and unloading the electrode interface capacitance [20]. The platinum electrode is a good example of polarizable electrode. By contrast, nonpolarizable electrodes pass current directly through the electrode-electrolyte interface [20] via oxidation-reduction reactions. The Ag/AgCl electrode is a good example of a nonpolarizable electrode. Accordingly charge displacement (for polarizable electrodes) or true charge transfer (for nonpolarizable electrodes) would occur when an electrode is placed near a source or sink of a dipole generated by a neuron or set of neurons during electrochemical changes associated with action potential generation (i.e., conductance of K^+ and Na^+).

The recorded electrode tip impedance varies with the AC frequency used to test the electrode [20, 22] (Fig. 1.3c), with high frequencies experiencing less impedance and low frequencies experiencing more opposition to current flow. This is particularly important since high-impedance electrodes are used to measure high-frequency action potentials. However, this feature may make these electrodes less suitable for recording local field potentials, particularly because of the high-pass filtering properties of the electrodes. Low frequencies tend to load and saturate the electrode tip capacitance and restrict further charge transfer to the headstage. However, this may only affect signal amplitude when microelectrodes are used in combination with low-input-impedance headstages (in the <40 MΩ range) [13]. By contrast, nonpolarizable electrodes tend to be good at recording low-frequency potentials since charge is transferred directly to the recording equipment. An additional property of electrodes is that as they are dipped deeper and deeper into electrolyte or the brain, the impedance appears to drop [12] (Fig. 1.3d). This phenomenon is actually a consequence of shunt capacitance C_s along the shaft of the electrode [12]. Indeed, there is actually charge dissipation between the metals of the electrode across the electrode insulation to the extracellular space and to the ground. An obvious method to counteract this is to increase the quality of insulation with a low dielectric (low permittivity).

Chronology of Metal Microelectrode Development

Single and Multiconductor Electrodes

Glass microelectrodes filled with electrolytic solution preceded the invention of the metal microelectrodes for recording from single neurons and probably influenced the use of glass as an insulating material early in the development of wire microelectrodes. Metal electrodes appeared superior for long-term in vivo recording because they were strong and their conductor was metal rather than an ionic solution. The parameters which early physiologists were trying to optimize were as follows: low electrical impedance to minimize noise pickup, a small tip diameter to isolate single neurons, and sufficient rigidity to prevent breakage during the insertion into the nervous system [23]. Today, we would expand this list to include biocompatibility and stability of signal over long periods of time. Moreover, the ability to separate one neuron from a background of neurons was of essential interest for early electrophysiologists, since algorithms to sort neurons had yet to be invented. Figure 1.5 shows a chronology of the major microelectrode developments which will subsequently be discussed.

In 1951, Weale [23] heated a glass capillary tube and pulled, drawing out an insulation for an electrode. He then fed a fine silver wire down the tube to produce a tip at the end of the electrode. A similar method was used by Svaetichin [24] who pulled molten silver solder into a glass capillary to produce the electrode tip. Subsequently, Dowben and Rose [25] developed a low-impedance electrode by a similar method composed of a finely drawn capillary tube with a 50 % tin/50 % indium core. Electrodes were able to record deep thalamic neurons with amplitudes as high as 1.2 mV in a cat model. In 1959, Gesteland et al. [26] reported their methodology for constructing the Wood's metal electrode. Wood's metal is composed of bismuth, lead, tin, and cadmium and has a very low melting temperature (~70 °C). Gesteland et al. [26] pulled a glass capillary to a fine tip and forced a piece of Wood's metal wire down the center of the capillary. When the shank of the pipette tip was heated with a hot plate, the Wood's metal wire melted at one end, and it could be pushed from the back, along the capillary to the end, to form the tip of the electrode.

Probably, one of the most famous early microelectrodes is the lacquer-coated tungsten microelectrode used by Hubel [27]. Hubel's electrode was designed for the specific purpose of recording chronically from minimally restrained cats. The tungsten electrode was mainly selected for its durability. This durability permitted Hubel to produce sharp-tipped tungsten electrodes through electrolytic sharpening and also permitted passage of the electrode through the dura mater. With these electrodes, units were isolated ranging from 0.5 to 10 mV for extracellular recording and could be recorded for up to an hour in minimally restrained cats. Subsequently, Green [28] developed a stainless steel electrode which had the advantage of lower noise when compared to tungsten electrodes and could be used to mark the electrode site with deposits of iron, followed by histological verification with a Prussian blue reaction. Similar to those of Hubel, these electrodes could sometimes record

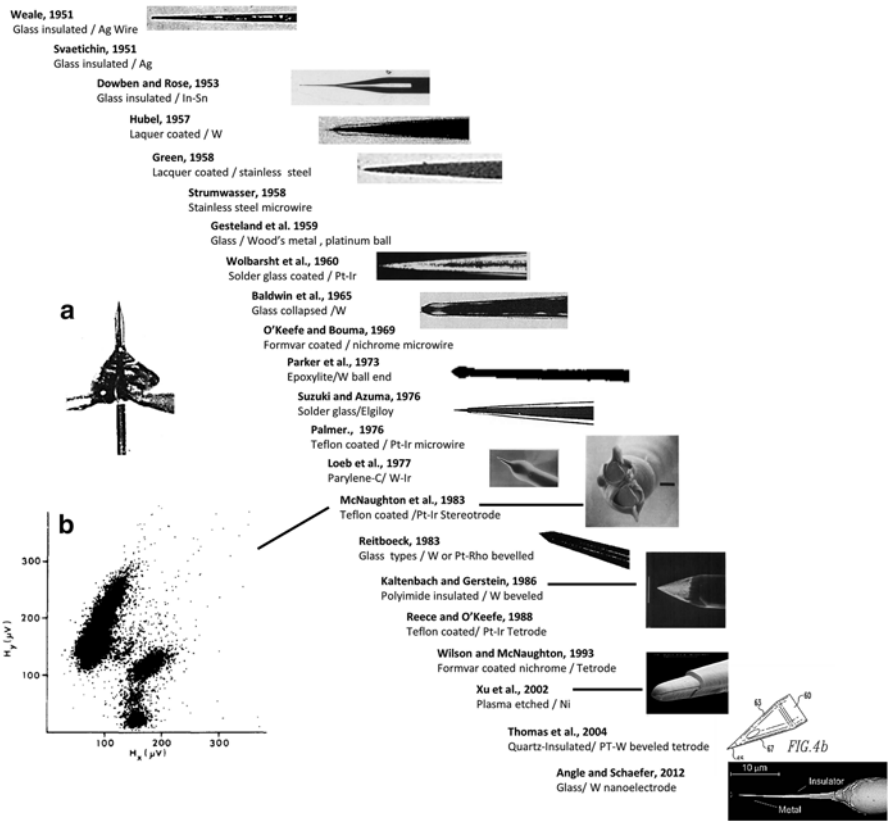

Fig. 1.5 Chronology of important microelectrode developments. The chronological development of metal microelectrode tips and their insulation from 1951 to 2012. Where possible, a photo is included of the actual electrode developed by the scientist. Under each reference is the insulation type and the conductor used (e.g., insulation/conductor). Reprinted with permission from Macmillan Publishers Ltd: Nature, Weale RA, A new micro-electrode for electrophysiological work, 167(4248), 529–30, copyright 1951. From Dowben RM, Rose JE. A metal-filled microelectrode. Science. 1953;118(3053):22–4. Reprinted with permission from AAAS. From Hubel DH. Tungsten Microelectrode for Recording from Single Units. Science 1957; 125(3247). Reprinted with permission from AAAS. Reprinted with permission from Macmillan Publishers Ltd: Nature, Green JD, A simple microelectrode for recording from the central nervous system, 182(4640), 962, copyright 1958. From Wolbarsht ML, Macnichol EF, Jr., Wagner HG. Glass Insulated Platinum Microelectrode. Science. 1960;132(3436):1309–10. Reprinted with permission from AAAS. From Baldwin HA, Frenk S, Lettvin. Glass-Coated Tungsten Microelectrodes. Science 1965; 148(3676). Reprinted with permission from AAAS. Reprinted from Electroencephalography and Clinical Neurophysiology, 35(6), Parker TD, Strachan DD, Welker WI, Tungsten ball microelectrode for extracellular single-unit recording, 647–51, Copyright 1973, with permission from Elsevier. Reprinted from Electroencephalography and Clinical Neurophysiology, 41(1), Suzuki H, Azuma M, A glass-insulated "Elgiloy" microelectrode for recording unit activity in chronic monkey experiments, 93–5, Copyright 1976, with permission from Elsevier. © 1977 IEEE. Reprinted, with permission, from Loeb GE, Bak MJ, Salcman M, Schmidt EM. Parylene as a chronically stable, reproducible microelectrode insulator. IEEE Trans Biomed Eng. 1977;24(2):121–8. Reprinted from Journal of Neuroscience Methods, 8(4),

10 mV extracellular spikes. Also notable was that in 1958, the first long-term (>1 day) neural recordings from an unrestrained animal conducted with a ground squirrel [29] using an 80 μm stainless steel microwires.

From this point, the evolution of the single fiber electrode took various twists and turns with modifications to tip geometry, insulations, and conductive materials. The first sharp-tipped platinum (70 %) and iridium (30 %) microelectrode was introduced by Wolbarsht et al. [30]. The electrodes were coated with molten solder glass using a heated loop (Fig. 1.5a). The next technical innovation came when Baldwin et al. [31] attempted to collapse a Pyrex glass capillary onto a fire-etched tungsten filament [31]. Finally O'Keefe and Bouma introduced the use of formvar-coated nichrome wires (25 μm core) for recording from the cat amygdala, which would later become a standard use in tetrodes [32].

In 1973, Parker et al. introduced a varnish (Epoxylite)-insulated tungsten ball electrode, which consisted of an electrode with a small ball 5–15 μm in diameter at the tip of the electrode [33]. The modification was thought to improve stability of the electrode in the brain and reduce damage from the otherwise sharp electrodes. Thereafter, this electrode did not become popular; however the necessity to solve the electrode stability problem persists today. The Elgiloy electrode was introduced by Suzuki and Azuma [34] and was composed of a nickel-cobalt alloy with about 15 % iron. These electrodes were insulated with solder glass and found to penetrate the monkey dura mater and record cells from microvolts well into the millivolts range. Concurrently, Palmer [35] was the first to publish the use of Teflon-coated 37 μm platinum-iridium microwires (90 % Pt/10 % Ir) to record cerebellar neurons in freely behaving animals. Importantly, the recorded cells could be held for up to a

Fig. 1.5 (continued) McNaughton BL, O'Keefe J, Barnes CA, The stereotrode: a new technique for simultaneous isolation of several single units in the central nervous system from multiple unit records, 391–7, Copyright 1983, with permission from Elsevier. Reprinted from Journal of Neuroscience Methods, 8(3), Reitboeck HJ, Fiber microelectrodes for electrophysiological recordings, 249–62, Copyright 1983, with permission from Elsevier. Reprinted from Journal of Neuroscience Methods, 16(4), Kaltenbach JA, Gerstein GL, A rapid method for production of sharp tips on preinsulated microwires, 283–8, Copyright 1986, with permission from Elsevier. Reprinted from Sensors and Actuators A: Physical, 96(1), Xu CY, Lemon W, Liu C, Design and fabrication of a high-density metal microelectrode array for neural recording, 78–85, Copyright 202, with permission from Elsevier. Courtesy of Thomas RECORDING in Giessen, Germany. Reproduced with permission from Angle MR, Schaefer AT. Neuronal recordings with solid-conductor intracellular nanoelectrodes (SCINEs). PLoS One. 2012;7(8):e43194. (**a**) The process of solder glass insulation, whereby a wire was repeatedly dipped into a bead of molten solder glass [30, 99]. With kind permission from Springer Science + Business Media: Medical and Biological Engineering, A Glass-Covered Platinum Microelectrode, 2, 1964, 317–27, Guld C. (**b**) Multiunit separation using a stereotrode. By comparing the amplitude of the units recorded simultaneously on wires X and Y of a stereotrode, a 2D projection can be made to separate neuron from neurons. Five obvious clusters (individual neurons) can be seen. Reprinted from Journal of Neuroscience Methods, 8(4), McNaughton BL, O'Keefe J, Barnes CA, The stereotrode: a new technique for simultaneous isolation of several single units in the central nervous system from multiple unit records, 391–7, Copyright 1983, with permission from Elsevier

week. Finally, in 1977, parylene C was introduced as an insulating material for tungsten and iridium electrodes. This process enabled precise tip exposures, and the material appeared to be very biocompatible, enabling scientists to isolate neurons from the monkey motor cortex for up to 100 days [36].

Until the 1980s the glass-coated sharp electrode held the spotlight for high-amplitude spike recordings, being able to pick up spikes from microvolts to millivolts. However, these electrodes weren't well equipped to sort multiunit activity. Indeed, multiunit activity was often considered a nuisance because of this difficulty. The sharp electrode was also not well noted for holding cells from day to day, especially in animals larger than a rat, where pulsation of the brain could influence electrode position. Finally, sharp electrodes suffered from an inability to discriminate cells in densely packed regions such as the hippocampus. Microwires, while not being able to penetrate the dura, had already shown evidence for stability in long-term recording [29]; however, microwires tend to detect small voltage signals (50–300 μV) and pick up an abundance of multiunit activity. Moreover their composition was such that they were difficult to implant, unless they were bundled together or reinforced. In spite of these apparent disadvantages, in 1983, McNaughton et al. [2] exploited some of these features as a primary advantage through the invention of the stereotrode. The stereotrode consisted of two Teflon-insulated 20 μm (75 % Pt/25 % Ir) wires twisted together and cut transversely with a pair of sharp scissors. The electrodes were simple and cost-effective, and the multiple conductors increased the strength of the electrode such that it could be implanted through the pial surface. The most important feature of the stereotrode was that the two wires of the stereotrode were spaced just microns apart so that each microwire could pick up signals from cells within and overlapping proximity. Thus, the same spike could be detected on both wires, but their spike sizes would not be the same. Accordingly, the spike amplitude for each covarying spike could be plotted with one spike represented on the *Y* axis and another spike on the *X* axis. This plot naturally forms clusters of neural data which can be grouped as statistically discrete spikes (Fig. 1.5b). While the conceptual advantage of the tetrode owes its inception to McNaughton et al., who suggested that a tetrahedral array would be optimal, the addition of the two extra microwires to the stereotrode to produce a tetrode owes credit to O'Keefe and Reece [37]. However, the most commonly used modern tetrode is the formvar nichrome (nickel and chrome) (40 μm total OD of the four wires) tetrode, introduced for large-scale hippocampus recording with multiple tetrodes [9].

In 1983 a quartz-coated platinum/rhodium electrode was produced which was beveled to a sharp point on a diamond grit grinding wheel [38]. The method for the platinum/rhodium electrodes was based on the Taylor wire method [39] for producing glass-coated wire and represented a substantial improvement in the reliable production of coated electrodes (often referred to as the Reitboeck electrode). Importantly, like the glass electrodes that preceded it, this electrode could penetrate the dura and drive straight through the brain tissue with minimal deviation. Quartz also has a lower dielectric constant than standard glass, so it acted as a better insulator. Finally, these electrodes were reported to have micro-striations or grooves on their

metal contacts which lowered electrode impedance. The German company, Thomas Recording later became known for the production and distribution of Thomas electrodes including a quartz-coated tetrode (see below).

The simple use of the grinding wheel to sharpen glass quartz-coated electrodes was also used by Kaltenbach and Gerstein [40] who sharpened polyimide-insulated tungsten microwire (25 μm). Thus, pre-insulated microwire technology began to cross-pollinate with that of the sharpened electrode technology.

In 2004 Thomas et al. [41] patented a 4-core quartz-insulated platinum (95 %) and tungsten (5 %) tetrode. This ~80 μm (OD) tetrode is beveled on a diamond grinding wheel and can be pulled thinner with the aid of a heating element. This electrode combines the best features of glass-coated electrodes with that of the pre-insulated microwire tetrode, effectively synthesizing the two most well-used historical techniques. Recently, a solid-conductor intracellular nanoelectrode (SCINES) has been constructed with a tungsten core conductor [42] and glass insulation. These electrodes were designed with the primary concern of puncturing the plasma membrane of neurons without producing leakage of current from the membrane. Puncturing or perforating membranes is nothing new for metal electrodes, dating back to Hubel's reports of sharpened tungsten electrodes. However, fluid-filled glass pipette electrodes have been the primary choice for intracellular recording, while extracellular recording is primarily done with metal electrodes. The SCINES electrode tip is milled microscopically with a focused ion beam to <300 nm. Shunt capacitance is reduced with special insulating procedures, and tips are coated with a hydrophobic compound "silane" to facilitate penetration into cells. These electrodes could pick up intracellular signals of a few millivolts including subthreshold neuronal potentials.

Microwire Electrode Arrays

As our understanding of electrochemistry and tip geometry of electrodes progressed so did the desire for large-scale neuronal recording. With increased numbers of neurons, we could examine neuronal activity simultaneously to study neuron-neuron communication and patterns of activity within the neural network. Early scientists used bundle electrodes to increase their potential neuron yield [32, 35, 43, 44] (Fig. 1.6a). However, simply offsetting the position of the individual wires in a bundle could produce a linear array of electrode contacts for which neurons could be detected across cortical layers and in different brain regions simultaneously.

One of the first notable designs of a linear array electrode was developed by Barna et al. [45]. This electrode array was constructed from a 30 gauge stainless steel hypodermic needle with a portion of the tube machined to half its width. Sixteen stainless steel microwires (25 μm) were passed through the tube, bent by 90°, and fixed to the side of the machined region (in the *Z* axis), with an interelectrode spacing of 400 μm (Fig. 1.6b).

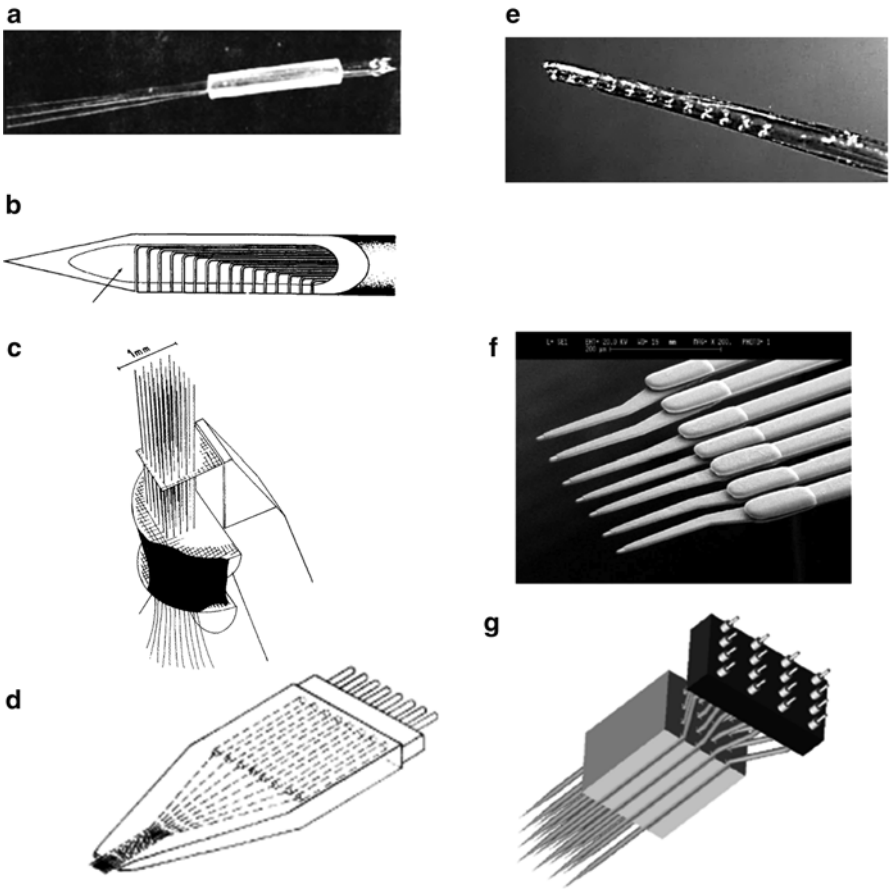

Fig. 1.6 Development of microelectrode arrays. (**a**) The bundled electrode preceded the array. This particular bundle was composed of sharpened tungsten electrodes and was implanted in humans [43]. Reprinted from Electroencephalography and Clinical Neurophysiology, 23(3), Marg E, Adams JE, Indwelling multiple micro-electrodes in the brain, 277–80, Copyright 1967, with permission from Elsevier. (**b**) Needle electrode linear array, electrodes are bent at 90° and clipped along the side of the 30G needle [45]. Reprinted from Electroencephalography and Clinical Neurophysiology, 52(5), Barna JS, Arezzo JC, Vaughan HG, Jr., A new multielectrode array for the simultaneous recording of field potentials and unit activity, 494–6, Copyright 1981, with permission from Elsevier. (**c**) Shows the three grids used to construct the 5×6 matrix of quartz-coated microelectrodes, and the bottom two grids are epoxied together to produce a substrate to hold the electrodes in parallel [46]. With kind permission from Springer Science+Business Media: Experimental brain research, Simultaneous recording with 30 microelectrodes in monkey visual, 41(2), 1981, 191–4, Kruger J, Bach M. (**d**) Parallel linear electrode array using metal microwires [47]. Reprinted from Journal of Neuroscience Methods, 11(3), Verloop AJ, Holsheimer J, A simple method for the construction of electrode arrays, 173–8, Copyright 1984, with permission from Elsevier. (**e**) Bundle array with 12 nichrome wire contacts [48]. Reprinted from Journal of Neuroscience Methods, 40(2, 3), Jellema T, Weijnen JA, A slim needle-shaped multiwire microelectrode for intracerebral recording, 203–9, Copyright 1991, with permission from Elsevier.

The first notable two-dimensional electrode array consisted of a 5×6 matrix of quartz-glass microelectrodes with platinum-iridium cores beveled to a fine tip and spaced at 160 μm [46] (Fig. 1.6c). Neurons were detected on at least 50 % of the implanted electrodes. Shortly thereafter, a parallel linear array was developed which consisted of eight 33 μm Karma wires spaced at 100 μm. This electrode array was primarily intended to record hippocampal field potentials [47] (Fig. 1.6d).

Jellema and Weijnen [48] developed a method for constructing a bundle array, consisting of 12 formvar-coated nichrome microwires (25 μm) embedded in Epoxylite resin with a 150 μm interelectrode spacing (Fig. 1.6e). This electrode array closely resembled styles of silicon probes at the time; however, as expressed by the authors, the silicon probe was financially prohibitive. The details of silicon probe techniques will be described in Chap. 2.

Eventually molding processes were used to enhance the feasibility of rapidly constructing electrode arrays [49]. However, with commercial metal electrode fabrication, the experimenter could focus on the experiment rather than on electrode and electrode array fabrication [50].

Xu et al. [51] combined fabrication techniques used in silicon chip production to produce a high-density metal microelectrode array (Fig. 1.6f). The basic concept was to electroplate the entire metal portion with nickel or permalloy (nickel-iron alloy). The second step was to remove silicon substrate to free the metal shanks of the electrode. The third phase was to add parylene C as an insulator for the electrodes. The tips of the electrodes were then exposed with photolithography followed by plasma etching, procedures commonly used in silicon chip manufacture.

Floating Wire Microelectrode

When recording from the neurons it would be best if we could track the life and experience of those neurons from days to years. This is seldom the case because there are pulsations of the brain, due to vascular supply and respiration, which change the position of the brain relative to the electrode. While this tends to be most prominent in larger vertebrates such as cats and primates, there is also the problem of bone growth which can gradually lift the secure electrode from its position in the brain. Indeed, it would only take a movement of 5 μm or less to significantly influence the amplitude of a recorded brain cell. This section focuses on floating

Fig. 1.6 (continued) (**f**) Electroplated parallel metal electrode array with silicon base [51]. Reprinted from Sensors and Actuators A: Physical, 96(1), Xu CY, Lemon W, Liu C, Design and fabrication of a high-density metal microelectrode array for neural recording, 78–85, Copyright 2002, with permission from Elsevier. (**g**) Shows a 4×4 matrix tungsten electrode array spaced by custom molds [49]. ©2005 IEEE. Reprinted, with permission, from Takahashi H, Suzurikawa J, Nakao M, Mase F, Kaga K. Easy-to-prepare assembly array of Tungsten microelectrodes. IEEE Trans Biomed Eng. 2005;52(5):952–6

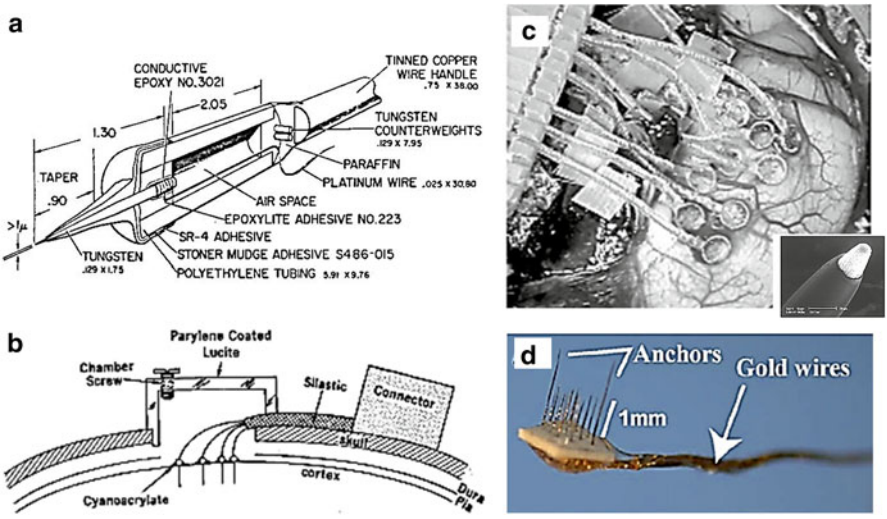

Fig. 1.7 Floating microelectrode technology. (**a**) First floating microelectrode device to record the frog vestibular system in outer space. Notice the air space, fine platinum wire, and counter weights, all used to minimize movements of the electrode relative to the body in which it was implanted. Reprinted from Electroencephalography and Clinical Neurophysiology, 25(1), Gualtierotti T, Bailey P, A neutral buoyancy micro-electrode for prolonged recording from single nerve units, 77–81, Copyright 1968, with permission from Elsevier. (**b**) Floating microwire electrodes free to move with pulsations of the brain and a chamber used to maintain cranial pressure and electrolytic interface. With kind permission from Springer Science + Business Media: Medical and Biological Engineering, A new chronic recording intracortical microelectrode, 14(1), 1976, 42–50, Salcman M, Bak MJ. (**c**) Pneumatically implanted sets of microelectrode arrays (circular pads) in the primate brain. Note the flexible leads to the left. The *bottom right inset* shows a scanning electron micrograph of the electrode tip. Reproduced with permission from Bradley DC, Troyk PR, Berg JA, Bak M, Cogan S, Erickson R, et al. Visuotopic mapping through a multichannel stimulating implant in primate V1. J Neurophysiol. 2005;93(3):1659–70. (**d**) Floating microelectrode array with anchor spikes. Reprinted from Journal of Neuroscience Methods, 160(1), Musallam S, Bak MJ, Troyk PR, Andersen RA, A floating metal microelectrode array for chronic implantation, 122–7, Copyright 2007, with permission from Elsevier

microelectrode devices which have been used in an attempt to match movements of the brain with that of the electrodes.

The first floating electrode was called a buoyancy microelectrode and owes its inception to Gualtierotti and Baily [52, 53]. This represented the first rational development of an electrode device which would move with nervous tissue (Fig. 1.7a). The tungsten electrode (Hubel design) used in this device was made buoyant because of an air pocket in the device for which it was attached. The device was additionally counterweighted, so the geometrical center of gravity was focused on the electrode. Finally, the electrode electrical connection was made with a small and flexible lead wire, so there would be minimal strain on the electrode when it was interfaced with the recording device. Electrical signals from the frog vestibular

nerve could be recorded from 2 to 5 days and during parabolic flights in a jet plane. These same floating electrodes were later used to study the vestibular system of the frog in outer space. It should be noted that 10 years earlier, Strumwasser [29] and Burns [54] demonstrated neuron stability from days to weeks using pre-insulated microwires.

Burns et al. [54] suggested that the movement of the electrode with time is dependent on the age and growth of the animal. Based on their estimates, a cat weighing 2.5 kg with an electrode at a depth of 3 mm would move 1.4 μm/day. By contrast, for a cat weighing 4.25 kg, the electrode would be expected to move 0.14 μm/day, as its growth rate will have slowed down. Collectively, it is likely that rigid electrodes such as those used by Hubel and the entire history of glass-coated electrodes, while having better ability to isolate single units, cannot hold these cells for prolonged periods of time because of their rigidity. Rigid electrodes do however have a significant advantage in that they are able to puncture dura. However, an intact dura should reduce brain pulsation and therefore prevent swelling and displacement of the electrode relative to the cell of interest.

Salcman and Bak [55] were the first to consider the consequence of craniotomy on electrode stability. They implanted a sharpened, floating, parylene C-insulated, 25 μm iridium microwire through the pia mater. The wires were glued to the pial surface with cyanoacrylate glue (Fig. 1.7b). The contact end of the electrode was secured to an ultra-flexible lead wire so the microwire could float with movements of the brain. Even more interesting was that the electrode leads were suspended in a fluid-filled chamber to reestablish the integrity of the cranial vault.

It was only a matter of time before the microelectrode array found an application in floating electrode technology. Bradley et al. implanted arrays of iridium microelectrodes into the monkey visual cortex [56] (Fig. 1.7c). The arrays of electrodes had a flexible lead so they could float on top of the pia. Thus the floating microelectrode technology had moved from a single electrode recording in the vestibular nerve of a frog to high-density electrophysiology in a primate. Musallam et al. [57] modified the floating microelectrode design not only to be more cost-effective but also to have anchor spikes which stabilized the array so that superficial cells could be recorded (Fig. 1.7d). It was found that neurons could be recorded in a rat up to 3 months after implantation.

Electrode Conditioning

Electrode impedance can be a major nuisance when recording with microelectrodes. The high impedances are a result of the small tip exposure of the microelectrodes. However, these small tips also make the electrode susceptible to picking up noise from the environment (e.g., 60 Hz hum).

Electroplating the electrode tip induces the growth of crystals on the electrode which has the effect of maintaining tip geometry while increasing tip surface area (e.g., Fig. 1.8a, b). The increased surface area reduces the tip impedance, resulting

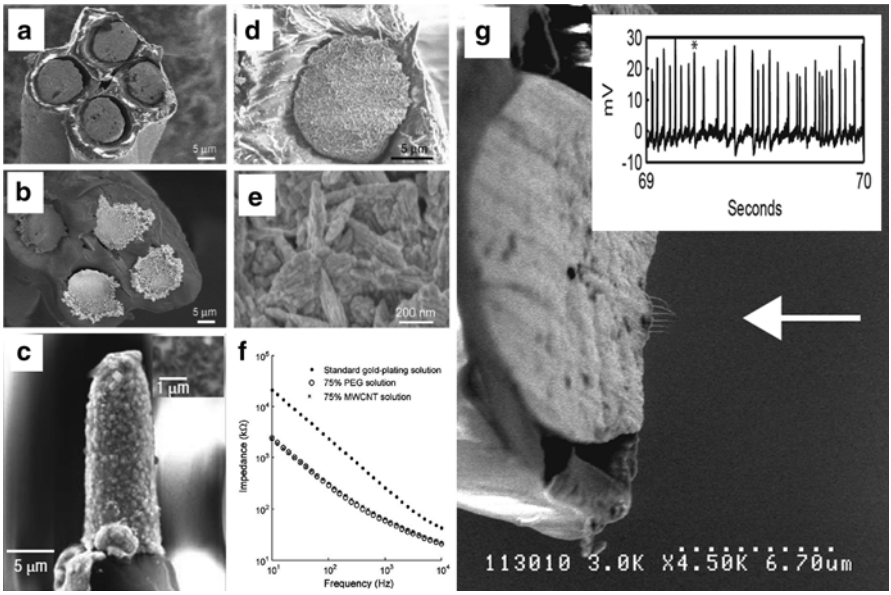

Fig. 1.8 Electrode conditioning. (**a**) Scanning electron micrograph of a tetrode before gold electroplating [62]. (**b**) Scanning electron micrograph of a tetrode after gold electroplating to 250 k**Ω** [62]. (**c**) Carbon nanotubes/gold attached to a tungsten microelectrode. Reprinted with permission from Macmillan Publishers Ltd: Nature Nanotechnology, Keefer EW, Botterman BR, Romero MI, Rossi AF, Gross GW, Carbon nanotube coating improves neuronal recordings, 3(7), 434–9, copyright 2008. (**d**) Tetrode tip plating has a "rice-like" appearance after electroplating with multiwalled carbon nanotubes [62]. (**e**) Magnified region of (**c**) showing "rice-like" coating is actually composed of bladed crystallites [62]. (**f**) Shows further decrease in impedance with electroplating with either of two additives, polyethylene glycol (PEG) or multiwalled carbon nanotubes (MWCNT) [62]. (**g**) Electron beam deposition of nanowires on the end of a single wire of a platinum-iridium electrode. *Inset* is intracellular recording from an intact T-cell neuron of a leech. Reproduced from Ferguson JE, Boldt C, Puhl JG, Stigen TW, Jackson JC, Crisp KM, et al. Nanowires precisely grown on the ends of microwire electrodes permit the recording of intracellular action potentials within deeper neural structures. Nanomedicine (Lond). 2012;7(6):847–53, with permission from Future Medicine Ltd. (**a**, **b**, **d**, **e**, and **f**) reprinted from Sensors and Actuators A: Physical, 156(2), Ferguson JE, Boldt C, Redish AD, Creating low-impedance tetrodes by electroplating with additives, 388–93, Copyright 2009, with permission from Elsevier

in less noise pickup from the environment. Electroplating is accomplished by the application of a current between an electrode and a plating solution (e.g., gold). A microampere DC current is passed through the microelectrode to attract the charged metal ion to the surface of the electrode. A reference electrode is also used to complete the circuit and to supply the solution with ions as they move from the solution to the plated microelectrode.

Svaetichin [24] has reported the use of platinum black to plate their silver microelectrodes. Dowben and Rose [25] later found that pre-plating their indium electrodes with gold could produce a base for which platinum black could be plated. Tungsten microelectrodes tend to be quite noisy, but plating with platinum followed

by gold reduces tip impedances [31, 58]. The gold pre-plating helps prevent platinum black from flaking off as the electrode penetrates through pia mater [59]. Robinson [59] noted that if an electrode is plated, the impedance will drop, but as time goes by, the impedance will gradually rise and experimenters often have to re-plate the electrodes just prior to use. The early introduction of the stereotrode consisted of a platinum-iridium wires that were plated with platinum to lower their impedance [2]. Soon thereafter, with the introduction of the nichrome tetrode, gold plating was used to reduce impedance [8]. Gold plating can reduce tetrode impedances from 1–2 MΩ down to 200 kΩ; however, if electrodes are over-plated, it has a tendency to short adjacent contacts within the tetrode tip. If reference and recording electrode impedances are precisely matched, most of the environmental noise is subtracted out with the differential amplifier. This can pose a problem for chronic recordings where the impedance of these electrodes may not remain stable with time.

One of the most successful methods of improving electrode impedance has been to electroplate electrodes in the presence of gold and carbon nanotubes using electrochemical techniques [60]. Carbon nanotubes have a high surface area and conductance, so they presumably make an ideal means of optimizing electrode tip impedance [61]. The mixture of carbon nanotubes in a gold solution could successfully coat stainless steel, tungsten single fiber electrodes (Fig. 1.8c), and tungsten stereotrodes. This coating appeared as a "rice-like" structure and significantly increased the ability to record neurons while decreasing the susceptibility to electrical noise. Subsequently, Ferguson [62] found that electroplating with the same additives as Keefer et al. [60] resulted in a "rice-like" shaped coating (Fig. 1.8d, e) and argued that the findings from Keefer were most likely to be a result of the carbon nanotubes absorbing into the electrode and acting as an inhibitor to gold plating. The result would be to limit the areas where the gold could plate the electrode, favoring the growth of new crystallites as opposed to the elaboration of previously plated crystals. Fergusson also used polyethylene glycol as a plating additive with gold and was able to produce the same rice-like structure while reducing electrode impedance (Fig. 1.8f). Finally, a combination of polyethylene glycol and carbon nanotubes with the gold solution produced a remarkably low-impedance electrode (30–70 kΩ). Although this may improve noise levels during recording it will only increase the resolution of far-field neurons.

Gesteland et al. [26] also noticed the benefit of additives for platinum microelectrode plating. They reported that the addition of gelatin to a platinum black solution produced a more adherent plating of platinum black on their Wood's metal electrode. With the invention of the quartz-insulated platinum/tungsten electrode, it was argued that the beveling procedure actually produces microgrooves [38] which reduce the impedance of the electrodes. As such they do not need to be plated prior to use; however some investigators do report gold plating to control their impedance [63]. Similar to tetrodes, single fiber tungsten, and stainless steel electrodes, effort has been made to coat Thomas electrode tips with carbon nanotubes to improve the signal-to-noise ratio. However, rather than use a mixture with gold, Baranauskas et al. [64] used a polypyrrole carbon nanotube composite. Similar to other composites, impedances were reduced between 1 and 10,000 Hz, with a dramatic increase in

signal-to-noise ratio in the 150–1,500 Hz range, which corresponds to the unit recording frequency band. Interestingly, consistent with Ferguson et al. [62], carbon nanotubes also appeared to increase the spike amplitude (from an average of 0.5 to 0.7 mV).

While lowering impedance of electrodes may reduce noise contamination, we need improvements in the opposite direction, toward stable high-density recording of high-amplitude spikes. We need clean signals from all the cells in a neural volume if we want to decode or predict the brain. Some interesting developments are starting to be seen in the field of nanotechnology. For example, what if nanowires could be grown on the tips of the electrode? Indeed, this concept is already being explored through the use of electron-beam-induced deposition to extend nanowires (microns long at 10–30 nm diameter) from the end of platinum-iridium electrodes [65] (Fig. 1.8g). Aluminum oxide was next laid down as an insulator, using an atomic layer deposition technique. Finally, a focused ion beam was used to mill the ends of the wires so as to expose their tips by removing the insulation and thereby producing impedances of around 1 MΩ. Remarkably, 15 mV potentials could be recorded from hippocampal slice preparations and 20 mV spikes from a leech preparation. We expect that approaches like this will pave the way for the future of metal microelectrode technology.

Chronology of Hyperdrive Development

The history of methods utilized to implant electrodes is one of diversity and innovation. The harpoon method was a common method to implant microwires, while the development of the hyperdrive in the 1970s came to be among the most common to independently move electrodes within the brain and can be used for either fine wire electrodes (e.g., tetrodes) or with single conductor electrodes.

Harpoons and Bundles

O'Keefe and Bouma [32] implanted their nichrome electrodes, fixed to a harpoon/probe with Carbowax (or polyethylene glycol). When the wax dissolved in the brain, the probe could be removed, leaving the electrodes in the surrounding tissue to detect neurons. Similarly, Burns et al. [54] inserted 30 μm platinum microwires through the dura by attaching the electrodes to a sharpened tungsten needle with sucrose. Westby and Wang's [66] approach was to use an array of microelectrodes attached with sucrose to a glass capillary. Remarkably, the investigators found that 81 % of their 252 implanted wires obtained neural recordings, many of which were still recording neurons 5 weeks later. As new methods for isolating neurons have been developed (below), the harpoon method for electrode insertion is rarely used.

Manual Microdrives

The microdrive was invented so that electrodes could be lowered into the brain in order to isolate new neurons. Early on, the term "microdrive" referred to the entire assembly of drive units [67]; it would later acquire the meaning of individual drive unit, while the term "hyperdrive" would refer to a set of microdrives. Because of these semantic issues, we will use the more modern terminology. A summary of many important hyperdrives and their schematics is shown in Fig. 1.9, the details for which we will discuss subsequently.

Blum and Feldman [67] invented a hyperdrive with independent movement of four electrodes for the study of the motor cortex of an anesthetized cat. The hyperdrive could be secured to a stereotaxic apparatus and consisted of four microdrives that could be independently driven by a micrometer. Soon after, Humphrey [68] invented a hyperdrive that closely approximates what we use today. This hyperdrive consisted of five microdrives, each driven by a mini setscrew which could advance the microdrive 277 μm/revolution against the force of a spring. The setscrews drove a piston that was attached to a tungsten electrode. The hyperdrive was intended for use with monkeys and cats and most remarkably was reported to be reloadable. Ainsworth and O'Keefe [69] had a similar design in which four drivescrews constituted the microdrive mechanism; however, instead of the drivescrews moving up and down, a drive nut would move up and down. The drive nut, tethered to the electrode, would move with the turn of the drivescrew (350 μm/revolution). Importantly, the drive was only 3 g, so it could be used for implantation in rats.

Other single microdrive units were introduced in the 1970s and appear to be adaptations of the design by Rank [70], the mechanism for which consisted of a screw which moved up and down inside a base [71]. The center of the screw was hollowed out, and the electrode was inserted through this hole [70]. The primary benefit of these drives was that they were small and could be used easily with rodents while awake or during sleep. However, the design features meant that electrodes turned with the drivescrew, which caused damage to the brain tissue and loss of neuron recording stability. There were various modifications made to this design, but only a few features are worth noting. Correction for rotation of the electrodes was explored by Deadwyler et al. [72] and Bland et al. [73], and the ability to replace electrodes was explored by Winson [71]. Finally, a design similar to Rank's drive was used to lower pre-insulated nichrome microwires into the brain for the first time in the hope of combining the best features of a floating electrode with those of a drivable electrode [74].

Another milestone was the development of the first purely actuated microdrive. This drive consisted of a screw that, when turned, drove a gear which was coupled to a geared linear post. Thus, rotational force was converted directly to linear actuation. This actuator was coupled to a glass-coated tungsten electrode which advanced 500 μm/revolution. It was capable of picking up stable units averaging 300–500 μV.

One of the most well-used microdrives was invented by Kubie et al. [44] and is still used today. The design consisted of ten 25 μm nichrome microwires which

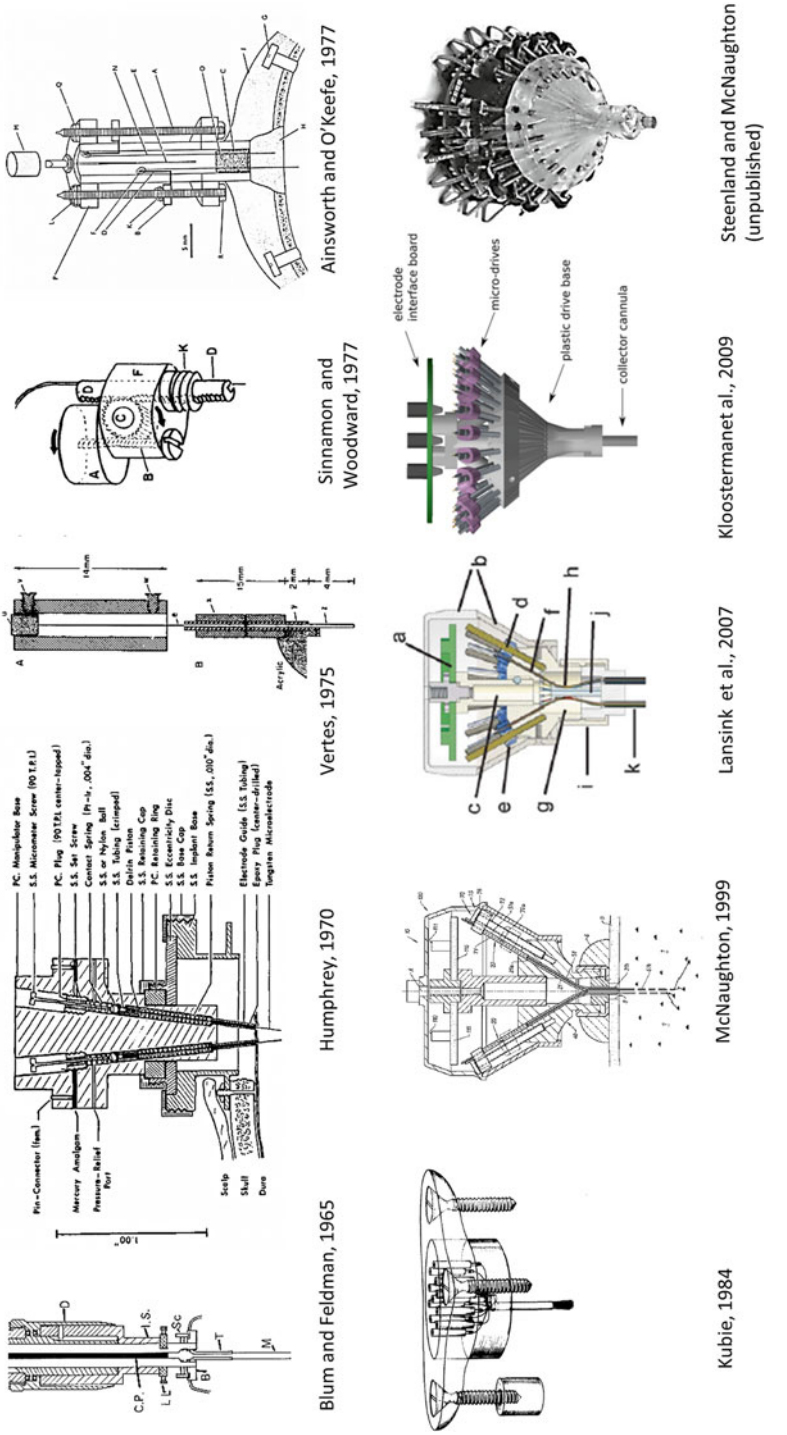
Blum and Feldman, 1965
Humphrey, 1970
Vertes, 1975
Sinnamon and Woodward, 1977
Ainsworth and O'Keefe, 1977
Kubie, 1984
McNaughton, 1999
Lansink et al., 2007
Kloostermanet al., 2009
Steenland and McNaughton (unpublished)
electrode interface board
micro-drives
plastic drive base
collector cannula

Fig. 1.9 Chronology of important manual hyperdrive developments. The manually driven hyperdrive evolved out of the combination of sets of microdrives. The microdrive mechanism commonly consisted of turning a thread which was coupled to the actuation of the electrode through a gear, nut, or shuttle. © 1965 IEEE. Reprinted, with permission, from Blum B, Feldman B. A microdrive for the independent manipulation of four microelectrodes. IEEE Trans Biomed Eng. 1965;12(2):121–2. Reprinted from Electroencephalography and Clinical Neurophysiology, 29(6), Humphrey DR, A chronically implantable multiple microelectrode system with independent control of electrode positions, 616–20, Copyright 1970, with permission from Elsevier. Reprinted from Electroencephalography and Clinical Neurophysiology, 38(1), Vertes RP, A device for recording single unit activity in freely-moving rats by a movable fine-wire microelectrode, 90–2, Copyright 1975, with permission from Elsevier. Reprinted from Physiology & Behavior, 19(3), Sinnamon HM, Woodward DJ, Microdrive and method for single unit recording in the active rat, 451–3 [100], Copyright 1977, with permission from Elsevier. Reproduced with permission from Ainsworth A, O'Keefe J. A lightweight microdrive for the simultaneous recording of several units in the awake, freely moving rat. J Physiol. 1977;269(1):8P–10P. Courtesy of John Wiley & Sons. Reprinted from Physiology & Behavior, 32(1), Kubie JL, A driveable bundle of microwires for collecting single-unit data from freely-moving rats, 115–8, Copyright 1984, with permission from Elsevier. McNaughton B, inventor; Implantable multi-electrode microdrive array. USA patent 5928143. 1999. Copyright Arizona Board of Regents for the University of Arizona. Reprinted from Journal of Neuroscience Methods, 162(1, 2), Lansink CS, Bakker M, Buster W, Lankelma J, van der Blom R, Westdorp R, et al., A split microdrive for simultaneous multi-electrode recordings from two brain areas in awake small animals, 129–38, Copyright 2007, with permission from Elsevier. Reproduced with permission from Kloosterman F, Davidson TJ, Gomperts SN, Layton SP, Hale G, Nguyen DP, et al. Micro-drive array for chronic in vivo recording: drive fabrication. J Vis Exp. 2009 [26]

were each bundled together in a stainless steel tube. The drive mechanism consisted of three independently drivable screws attached to a platform. Similar to Gualtierotti and Baily [52, 53], who invented the buoyancy electrode to study the vestibular system in outer space, Knierim et al. [75] explored the neuronal activity of the hippocampus, in zero gravity on a NASA flight, with a new hyperdrive design originally based on earlier designs from the same lab [9, 76]. The particular hyperdrive used for the NASA mission was constructed by Kopf instruments and later patented by Bruce McNaughton [7]. The major innovations in this drive are listed in its patent and include a circular array of 14 tetrodes that run parallel to one another and are orientated outwardly via guide tubes. Additionally, the microdrives consisted of tripods with a central nut connected to a threaded rod (fixed to the hyperdrive base). When the nut was turned, the microdrive moved, guided linearly by the two legs and the threaded rod. Thus, electrodes fixed in these drives could be moved forward with a turn of the nut and be guided into the brain by the array of guide tubing. This drive was later redesigned to include an additional electrode bundle so that two brain regions could be simultaneously targeted [77].

Kloosterman et al. [78] published a fabrication protocol for a hyperdrive which was designed with SolidWorks software and could be made from plastic, using 3D stereolithography printing process. The flexibility of the design software in combination with the printing process will permit easy customization of hyperdrives at a reasonable cost in years to come. The Kloosterman drive shares many features with the Kopf drive; however, the microdrive mechanism is a di-pod rather than a tripod. Moreover, the threaded screw which moves the microdrive downward actually moves via tapped threads arrayed around the drive. A more recent development in our laboratory (unpublished) using the Kloosterman drive involves the use of flexible connections between each microdrive and a specialized hyperdrive electrode interface board. This flexible connection permits us to reload standard tetrodes or Thomas quartz-insulated electrodes into rats, should the older electrodes begin to fail. Such flexibility is expected to increase neuron yield and long-term use of the subject under study.

While most of the drive styles listed above were designed for rats or larger animals, there remained a major problem with recording from smaller animals such as birds and mice. Given the enthusiasm for genetic work in mice, the design of drives to suit these ends were also required. Korshunov developed a 120 mg mini-microdrive module to be used with sharp microelectrodes in freely behaving mice and baby chicks. The microdrive mechanism consisted of a module for which linear movement (250 μm revolution) of the electrode occurred through turning a threaded drive tube. With similar technology, Korshunov also developed the first waterproof microdrive system so animals could be tested in the Morris water maze [79], even while submerged underwater. Many microdrives for mice and rats are also available from neuroscience vendors. However, with an increasing focus on the study of distributed networks and the integration of optogenetic and pharmacological technologies, the need for flexible, in-house design is again growing, supported by modern modeling software (e.g., SolidWorks) and fabrication processes (e.g., stereolithography).

Rotary Motorized Hyperdrives

Many hyperdrives use rods or threaded screws as the means to move parts of the microdrive up and down. However, all of the hyperdrives reviewed thus far require the experimenter to manually turn the microdrive mechanism. Some investigators have taken the approach of motorizing the microdrive mechanism. The advantage is that the animal under study doesn't need to be restrained in order to move the electrodes. Furthermore, the precision of actuation and the isolation of neurons would be improved. The downside is the cost and the weight of the device to be carried on the animal's head. A summary of the important rotary motorized hyperdrives and their schematics is shown in Fig. 1.10, the details of which we will discuss subsequently.

Findlay [80] devised an early DC motorized microdrive for freely behaving cats and rabbits. The motor terminated in a worm and pinion gear to actuate the electrode up and down in a linear fashion. The motor could be controlled remotely and could advance the electrode by a mere 1.25 μm. Subsequently, Barmack et al. [81] developed a microdrive that was driven directly by a stepper motor and was intended for primate work. The advantage of stepper motor drives over DC style drives is that each step is very precise. Fee and Leonardo [82] set out to miniaturize the motorized microdrive for small animals such as mice and small song birds which can lift about 2–5 g of weight on their skulls. Their finished product weighed around 3 g and consisted of three independently drivable DC mini-motors. Each of the three motors could be independently controlled, and the motor was directly coupled to a threaded rod which drove a shuttle. The shuttle moved up and down linearly as the threaded rod turned (~160 μm/turn) and drove the electrode (fine sharp tungsten) into the brain. The examples of unit isolation reported by Fee and Leonardo [82] were between 1 and 4 mV reaching up to 10 mV, orders of magnitude higher than pre-insulated fine wire electrodes. Just as remarkable was that if the amplitude of the cell recording drifted, the electrodes could be readjusted without touching the animal under study.

Yamamoto and Wilson [83] substantially expanded upon the mini-motorized microdrive technology that Fee and Leonardo [82] had introduced. The authors introduced three new major features. First, they found a way to multiplex the signals that drive the motors, which cut down on weight and cabling to the animals head when the drive was implanted. The second feature was to increase the number of motors for the mouse style hyperdrive (4.8 g) to 7 while the rat microdrive (29 g) had 21. Third, the microdrive base was constructed using a stereolithography technique which meant that the device could be constructed from strong lightweight material. The drive could move a tetrode in steps as small 0.6 μm. The largest spikes reported were approximately 2.35 mV, which is 4.25× lower than those reported by Fee and Leonardo, possibly owing to the use of a blunt tetrode rather than a sharp electrode.

While motorized hyperdrives have come a long way from their original inception, the cost of production for these devices is high, and the parts involved are

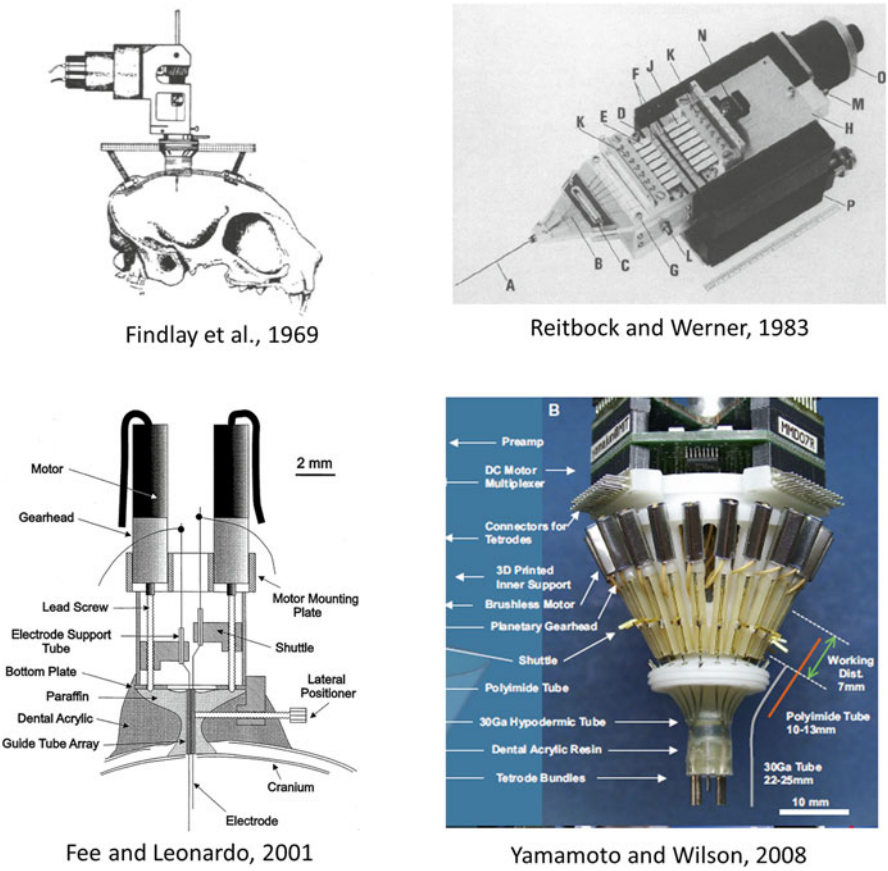

Fig. 1.10 Rotary motorized hyperdrives. Developments of motorized drives to increase the precision of neuron isolation. Such drives also permit the experimenter to manipulate electrode depth without directly interacting with the animal. Reproduced with permission from Findlay AL, Horn G, Stechler G. An electrically operated micro-electrode drive for use on unanaesthetized animals. J Physiol. 1969;204(1):4P–6P. Courtesy of John Wiley & Sons. With kind permission from Springer Science + Business Media: Experientia, Multi-Electrode Recording-System for the Study of Spatio-Temporal Activity Patterns of Neurons in the Central Nervous-System, 39(3), 1983, 339–41 [101], Reitbock HJ, Werner G. Reprinted from Journal of Neuroscience Methods, 112(2), Fee MS, Leonardo A, Miniature motorized microdrive and commutator system for chronic neural recording in small animals, 83–94, Copyright 2001, with permission from Elsevier. Reproduced with permission from Yamamoto J, Wilson MA. Large-scale chronically implantable precision motorized microdrive array for freely behaving animals. J Neurophysiol. 2008;100(4):2430–40

delicate (e.g., motors). They also add substantially to the weight of the hyperdrive. Should hyperdrives become more useful for doing intracellular recording with nanowires or juxtacellular recording, it should be expected that the motorized hyperdrives will be essential for precision control. However, unless DC or stepper motors can be made smaller and of lighter weight while retaining their torque, it may be of interest to look toward piezoelectric motors.

Piezomotor Hyperdrives

Piezoelectric motors are now becoming incredibly popular, probably in part due to their involvement in focusing lenses for the smartphone industry. The piezocrystal shape becomes distorted when a voltage is dropped across it. This distortion can be harnessed to create motion. Linear motion peizomotors eliminate the need for using threaded screws and gears to couple rotation to linear actuation in the microdrive. Moreover, peizomotor motion or steps can be incredibly small with nanometer resolution. This section will discuss some of the recent advances in piezomotor hyperdrive development.

Cham et al. [84] used a linear actuating piezomotor hyperdrive for semi-chronic use in primates with sharp platinum-iridium electrodes (Fig. 1.11a). In addition, the authors integrated an autonomous control algorithm so that a computer could isolate the neurons through driving the piezoelectric motor and checking the resulting spike signals (Fig. 1.11b). The only drawback with these motors, as with any motors, is the electrical noise they produce on the recording electrode when actuating. Park et al. [85] improvised a single piezoelectric microdrive (5 g) for mice and found it helpful for the micro-positioning of their electrodes. The idea was later improved by Yang et al. [86, 87] by using a more practical piezoelectric motor, reducing the weight to 1.82 g, and integrating a position feedback system (Fig. 1.11c). Yang et al. [86] found that micro-positioning of the tetrodes (<5 μm) was sufficient to increase the number of clustered units within the tetrode recording (Fig. 1.11d). In addition, the minimum step of the piezoelectric motor was 1 μm, and the electrical noise generated by actuation was negligible for recording purposes. However, this drive was still only able to position a bundle of tetrodes without the independent manipulation of the tetrodes. In the future this style of drive can be extended to produce a hyperdrive for remote control of electrode positions in high-density electrophysiology.

High-Density Electrophysiology and Stimulation

In vivo multiunit electrophysiology has been combined with behavioral manipulations for the past 60 years. In contrast, in vitro experiments involve local manipulations but do not consider the context of the behaving animal. Neither of these methods can completely reverse engineer the brain. An effective engineering approach relies on the local ability to manipulate parts of a system and see both local and global effects of the system. The following section will examine attempts to systematically manipulate local regions of the brain while simultaneously monitoring neuron responses in vivo.

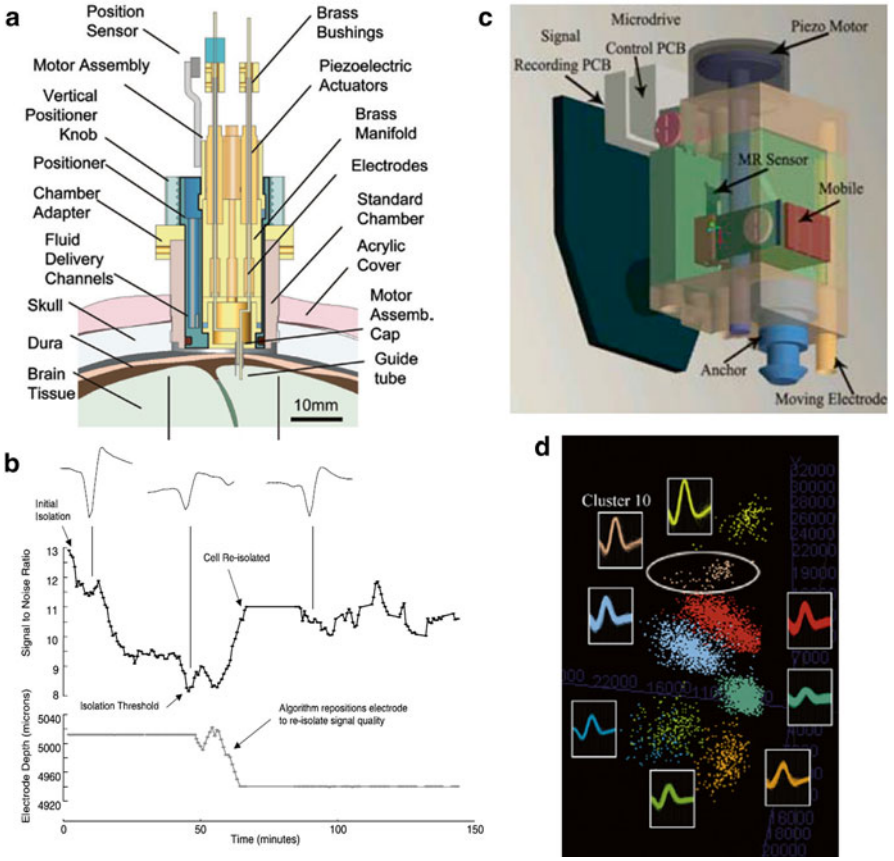

Fig. 1.11 Piezomotor hyperdrives. (**a**) Cross section through a piezomotor hyperdrive with independent motion of four motors, a sensor is used to calculate the position that the electrodes have actuated. Note there are no gears or threaded rods, just a piezomotor coupled to an electrode. Reproduced with permission from Cham JG, Branchaud EA, Nenadic Z, Greger B, Andersen RA, Burdick JW. Semi-chronic motorized microdrive and control algorithm for autonomously isolating and maintaining optimal extracellular action potentials. J Neurophysiol. 2005;93(1):570–9. (**b**) Results of an autonomous algorithm, used to control the positioning of the electrode depth to optimize the signal-to-noise ratio of particular spikes. Algorithm was used to control the hyperdrive in (**a**). Reproduced with permission from Cham JG, Branchaud EA, Nenadic Z, Greger B, Andersen RA, Burdick JW. Semi-chronic motorized microdrive and control algorithm for autonomously isolating and maintaining optimal extracellular action potentials. J Neurophysiol. 2005;93(1):570–9. (**c**) Example of a piezoelectric microdrive for moving a single electrode bundle in mice. © 2008 IEEE. Reprinted, with permission, from Yang S, Lee S, Park K, Jeon H, Huh Y, Cho J, et al. Piezo motor based microdrive for neural signal recording. Conf Proc IEEE Eng Med Biol Soc. 2008;2008:3364–7. (**d**) Tetrode recording with a piezoelectric microdrive in mice. The *circle* around the clustered cell represents a new cluster which was isolated with actuation of the piezomotor by just 4 **μ**m. Reprinted from Journal of Neuroscience Methods, Vol/edition number, Yang Y, Cho J, Lee S, Park K, Kim J, Huh Y, Yoon E-S, et al., Feedback controlled piezo-motor microdrive for accurate electrode positioning in chronic single unit recording in behaving mice, 117–127, Copyright 2011, with permission from Elsevier

Drug Delivery and Spike Recording

Pharmacology is among the most well-used methods employed to manipulate local brain regions while simultaneously monitoring behavior. However, in spite of this advantage, there is a paucity of literature combining pharmacology with high-density electrophysiology. This is in part due to the lack of effective drug delivery strategies that do not also produce pressure artifacts on neuron recording (e.g., microinjection). In addition, local manipulation does not always influence behavior, since the drug may not spread far enough. Finally, the specificity of drug manipulations depends on the quality of the pharmacological agents. A method which has been rather underused is that of reverse microdialysis. A microdialysis probe consists of a fluid inlet and outlet and a semipermeable membrane probe tip interposed between the inlet and outlet (Fig. 1.12a). With this method, drugs can be delivered without increasing local pressure around the tip of the probe.

Early attempts to combine microdialysis with electrophysiology revolved around local field potential and seizure manipulations [88]. However, designs began to incorporate bundles of microwires implanted adjacently to the microdialysis probes. For example, Ludvig et al. used a Kubie drive to position microwires and a dialysis probe in the hippocampus [89] (Fig. 1.12b, c). This electrode-microdialysis configuration could record up to 3 days in freely behaving animals. Once the electrode and probe were lowered into the hippocampus, the investigators found that they could both activate and deactivate neurons when the perfusion solution was switched to either high potassium or lidocaine, respectively (Fig. 1.12d, e). Moreover, in some cases, all eight electrodes could record neural activity, while perfusion solutions were switched. Subsequently, a Kubie style microdialysis multiunit drive was developed for use in primates [90], and recent advances have combined the Gothard-McNaughton style hyperdrive [76] with microdialysis for studies in rats [91].

By far, one of the major limitations to microdialysis is lag time for the drug to reach the probe tip. When a solution is switched from artificial cerebral spinal fluid (control) to a drug, the drug must be pumped through tubing from that switch to the microdialysis probe; this can take between 5 and 10 min. In 2002, Ludvig et al. [92] invented a device for rapid switching of perfusion solutions. The basic concept is to have both the perfusion solution and the drug pumped through separate channels to a switch located on the animal's head. Under these conditions, drugs could be delivered rapidly (within 1 min) of switching to the solution of interest.

Optical Stimulation and Spike Recording

The excitement for the optogenetic approach has become widespread. Optogenetics involves using light to activate light-sensitive channels (e.g., channelrhodopsin-2) which have been expressed in specific neurons [93]. Activating these channels permits specific manipulations of the neurons at on the millisecond timescale [94].

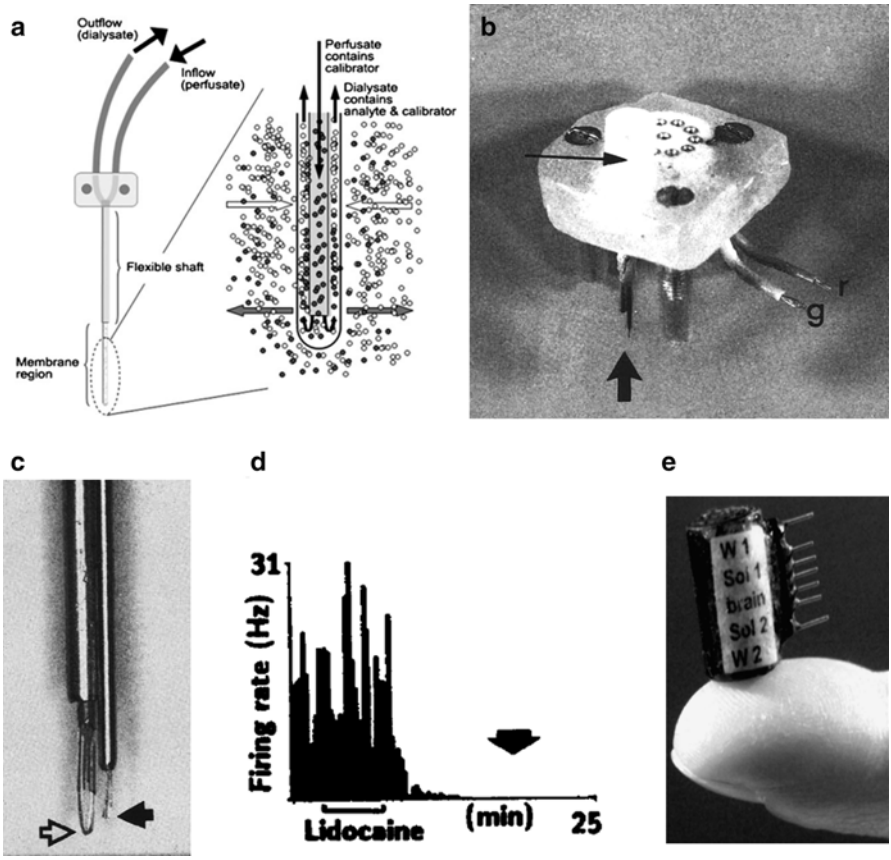

Fig. 1.12 Combined microdialysis and spike recording. (**a**) Example of a microdialysis probe. The inlet feeds to a semipermeable membrane which permits higher concentration compounds to pass into the brain. The outlet relieves pressure. With kind permission from Springer Science + Business Media: Pharmaceutical Research, AAPS-FDA workshop white paper: microdialysis principles, application and regulatory perspectives, 24(5), 2007, 1014–25 [102], Chaurasia CS, Muller M, Bashaw ED, Benfeldt E, Bolinder J, Bullock R, et al. (**b**) Combination of Kubie microdrive with microdialysis probe. The three screws around the perimeter are used to actuate the wires and microdialysis probe into the brain [89]. (**c**) Close-up of the microwire bundle and the dialysis probe tip (spaced 500 **μ**m apart) [89]. (**d**) Neural response to dialysis of lidocaine in the vicinity of the microwire electrodes. Washout with ACSF did lead to full recovery of neural responses [89]. (**e**) Rapid fluid switches which can be attached to the skull of freely behaving animals. Outermost tubes are air valves for opening and closing connection to the "brain." Two tubes are used as return lines to wash (W) drug out. Two tubes are used to preload solutions (Sol) (e.g., ACSF and drug [92]). Reprinted from Brain Research Protocols, 9(1), Ludvig N, Kovacs L, Kando L, Medveczky G, Tang HM, Eberle LP, et al., The use of a remote-controlled minivalve, carried by freely moving animals on their head, to achieve instant pharmacological effects in intracerebral drug-perfusion studies, 23–31, Copyright 2002, with permission from Elsevier. (**b–d)** Reprinted from Journal of Neuroscience Methods, 55(1), Ludvig N, Potter PE, Fox SE, Simultaneous single-cell recording and microdialysis within the same brain site in freely behaving rats: a novel neurobiological method, 31–40, Copyright 1994, with permission from Elsevier

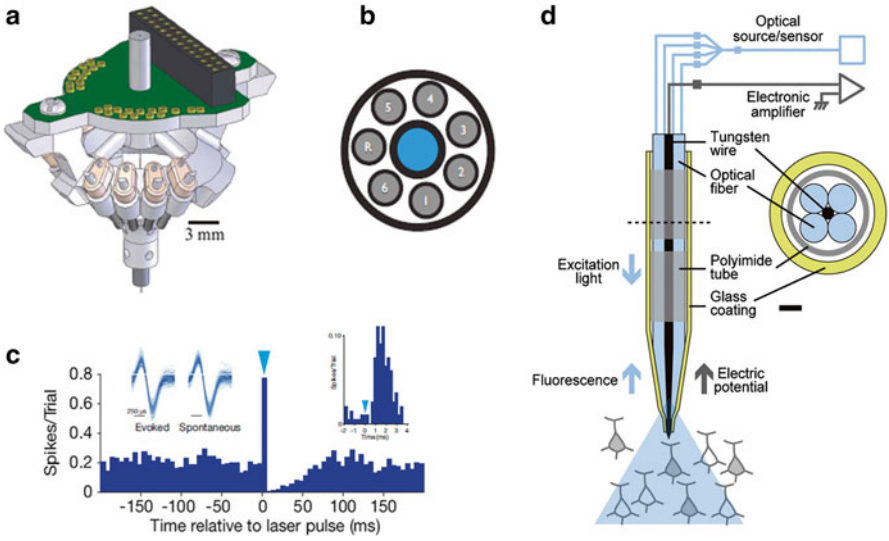

Fig. 1.13 Combined optogenetics and spike recording. (**a**) Example of an optogenetic hyperdrive with six tetrode recording channels and one reference electrode. Fiber optic is driven through the center of the hyperdrive [95]. (**b**) Cross-section through the drive bundle showing orientation or electrode positions and that of the optical fiber [95]. (**c**) Stimulation of inhibitory neurons expressing channelrhodopsin-2 inhibits firing of locally recorded neurons [95]. (**a**–**c**) © 2011 IEEE. Reprinted, with permission, from Siegle JH, Carlen M, Meletis K, Tsai LH, Moore CI, Ritt J. Chronically implanted hyperdrive for cortical recording and optogenetic control in behaving mice. Conf Proc IEEE Eng Med Biol Soc. 2011;2011:7529–32. (**d**) Glass-coated electrode composite of four optical fibers and one central sharp tungsten electrode. This electrode was capable of exciting channelrhodopsin while detecting fluorescent emission spectra (from EYFP). Emission was used to determine the proximity to channelrhodopsin-2 expressing regions in the primate thalamus. Reprinted from Journal of Neuroscience Methods, 211(1), Tamura K, Ohashi Y, Tsubota T, Takeuchi D, Hirabayashi T, Yaguchi M, et al., A glass-coated tungsten microelectrode enclosing optical fibers for optogenetic exploration in primate deep brain structures, 49–57, Copyright 2012, with permission from Elsevier

Siegle et al. [95] were the first to develop a hyperdrive capable of simultaneous optogenetic stimulation and high-density electrophysiology in mice (Fig. 1.13a). The drive was constructed with stereolithography, and an optical fiber was positioned in the middle of the hyperdrive with six recordings and one reference electrode concentrically placed around it (Fig. 1.13b). The optical fiber was set to shine into the brain from the cortical surface, and specific interneurons were engineered to carry the channelrhodopsin-2 protein. Importantly, light stimulation was found to inhibit recorded neurons, presumably through activation of these inhibitory neurons (Fig. 1.13c).

The hyperdrive described above is an excellent start for using optogenetics in high-density electrophysiology; however the spatial selectivity of the fiber optic is rather lacking, because it relies only on particular neurons that express the channelrhodopsin. Additional spatial selectivity might be added by designing recording

microelectrodes with an integrated fiber optic. Tamura et al. [96] designed a glass-coated, four-channel fiber optic and one-channel tungsten microelectrode, so that stimulation and recording could be conducted with the same electrode. The construction of this electrode borrowed the 1970s techniques for collapsing glass capillary over the tungsten electrode [58, 97] using an electrode puller. Figure 1.13d shows an example of the final construction, with the sharpened tungsten electrode core oriented at the center and four optical fibers orientated around it. Not only could this electrode activate cells expressing channelrhodopsin in primates, it could also detect emission spectra from fluorescent YFP tagged neurons when the laser light was shone on them. Using this emission, the authors could dial their electrode down to the approximate location for which neurons expressed both the channelrhodopsin and fluorescent protein. This electrode design has incredible potential for large-scale electrophysiology. If this electrode composite could be miniaturized and made flexible, it might be suitable for loading into a hyperdrive. Moreover, the ability to excite silent cells in the vicinity of the electrode may help solve the problem of why so few cells get recorded when there are such dense populations surrounding the electrode. Finally, there is a need to invent a fiber-optic tetrode, which may permit the dissection of local circuit connectivity.

Summary

This review serves as a substrate to understand the history and synthesis of technical developments for metal microelectrode over the past 60+ years. Many theoretical issues have advanced, including our understanding of the electrode-electrolyte interface and how best to condition electrodes. After 60 years of exploration, both the pre-insulated microwire and the glass-coated electrode still persist, and new outlets in optogenetics and developments in nanotechnology are being discovered. Hyperdrives have been revised numerously, and in some inceptions incorporate motors and piezoelectric actuators for precision movement of electrodes. Moreover, hyperdrive construction has been made entirely flexible through the use of stereolithography. We are encountering a new age of large-scale electrophysiology, in which simultaneous manipulation and recording of intracellular and extracellular neurons in vivo will combine seamlessly with pharmacology and optogenetics.

Acknowledgments Special thanks to Mary Steenland, Sara-Lynn Pelegrin, Erik Hopkins, and Dr. Masami Tatsuno for a careful editing of this chapter.

References

1. Szabo I, Marczynski TJ. A low-noise preamplifier for multisite recording of brain multi-unit activity in freely moving animals. J Neurosci Methods. 1993;47(1–2):33–8. Epub 1993/04/01.
2. McNaughton BL, O'Keefe J, Barnes CA. The stereotrode: a new technique for simultaneous isolation of several single units in the central nervous system from multiple unit records. J Neurosci Methods. 1983;8(4):391–7. Epub 1983/08/01.

3. Fee MS, Mitra PP, Kleinfeld D. Automatic sorting of multiple unit neuronal signals in the presence of anisotropic and non-Gaussian variability. J Neurosci Methods. 1996; 69(2):175–88. Epub 1996/11/01.
4. Einevoll GT, Franke F, Hagen E, Pouzat C, Harris KD. Towards reliable spike-train recordings from thousands of neurons with multielectrodes. Curr Opin Neurobiol. 2012;22(1):11–7. Epub 2011/10/26.
5. Aika Y, Ren JQ, Kosaka K, Kosaka T. Quantitative analysis of GABA-like-immunoreactive and parvalbumin-containing neurons in the CA1 region of the rat hippocampus using a stereological method, the dissector. Exp Brain Res. 1994;99(2):267–76. Epub 1994/01/01.
6. Henze DA, Borhegyi Z, Csicsvari J, Mamiya A, Harris KD, Buzsaki G. Intracellular features predicted by extracellular recordings in the hippocampus in vivo. J Neurophysiol. 2000;84(1):390–400. Epub 2000/07/19.
7. McNaughton B, inventor. Implantable multi-electrode microdrive array. USA patent 5928143. 1999.
8. Gray CM, Maldonado PE, Wilson M, McNaughton B. Tetrodes markedly improve the reliability and yield of multiple single-unit isolation from multi-unit recordings in cat striate cortex. J Neurosci Methods. 1995;63(1–2):43–54. Epub 1995/12/01.
9. Wilson MA, McNaughton BL. Dynamics of the hippocampal ensemble code for space. Science. 1993;261(5124):1055–8. Epub 1993/08/20.
10. Terzuolo CA, Araki T. An analysis of intra- versus extracellular potential changes associated with activity of single spinal motoneurons. Ann N Y Acad Sci. 1961;94:547–58. Epub 1961/09/06.
11. Clark J, Plonsey R. The extracellular potential field of the single active nerve fiber in a volume conductor. Biophys J. 1968;8(7):842–64. Epub 1968/07/01.
12. Robinson DA. Electrical properties of metal microelectrodes. Proc IEEE. 1968;56(6): 1065–71.
13. Nelson MJ, Pouget P, Nilsen EA, Patten CD, Schall JD. Review of signal distortion through metal microelectrode recording circuits and filters. J Neurosci Methods. 2008;169(1):141–57. Epub 2008/02/05.
14. Geddes LA, Baker LE. Principles of applied biomedical instrumentation. New York: Wiley; 1968.
15. Leung L. Field potential generation and current source density analysis. In: Walz W, editor. New York: Springer; 2010.
16. Rosenthal F, Woodbury JW, Patton HD. Dipole characteristics of pyramidal cell activity in cat postcruciate cortex. J Neurophysiol. 1966;29(4):612–25. Epub 1966/07/01.
17. Leung S. Field potential generation and current source density analysis. In: Walz W, editor. Springer; 2011.
18. Rosenthal F. Extracellular potential fields of single PT-neurons. Brain Res. 1972;36(2): 251–63. Epub 1972/01/28.
19. Beaulieu C, Colonnier M. Effects of the richness of the environment on six different cortical areas of the cat cerebral cortex. Brain Res. 1989;495(2):382–6. Epub 1989/08/28.
20. Neuman MR. Chapter V: Biopotential electrodes. In: Webster JG, editor. Medical instrumentation application and design. 4th ed. New York: Wiley; 2010.
21. Riistama J, Lekkala J. Electrode-electrolyte interface properties in implantation conditions. Conf Proc IEEE Eng Med Biol Soc. 2006;1:6021–4. Epub 2007/10/20.
22. Geddes LA, Da Costa CP, Wise G. The impedance of stainless-steel electrodes. Med Biol Eng. 1971;9(5):511–21. Epub 1971/09/01.
23. Weale RA. A new micro-electrode for electrophysiological work. Nature. 1951; 167(4248):529–30.
24. Svaetichin G. Electrophysiological investigations on single ganglion cells. Acta Physiol Scand Suppl. 1951;24(86):1–57. Epub 1951/01/01.
25. Dowben RM, Rose JE. A metal-filled microelectrode. Science. 1953;118(3053):22–4. Epub 1953/07/03.
26. Gesteland RC, Howland B, Lettvin JY, Pitts WH. Comments on microelectrodes. Proc IRE. 1959;47(11):1856–62.

27. Hubel DH. Tungsten microelectrode for recording from single units. Science. 1957;125(3247):549–50. Epub 1957/03/22.
28. Green JD. A simple microelectrode for recording from the central nervous system. Nature. 1958;182(4640):962. Epub 1958/10/04.
29. Strumwasser F. Long-term recording' from single neurons in brain of unrestrained mammals. Science. 1958;127(3296):469–70. Epub 1958/02/28.
30. Wolbarsht ML, Macnichol Jr EF, Wagner HG. Glass insulated platinum microelectrode. Science. 1960;132(3436):1309–10. Epub 1960/11/04.
31. Baldwin HA, Frenk S, Lettvin JY. Glass-coated tungsten microelectrodes. Science. 1965;148(3676):1462–4. Epub 1965/06/11.
32. O'Keefe J, Bouma H. Complex sensory properties of certain amygadala units in the freely moving cat. Exp Neurol. 1969;23(3):384–98. Epub 1969/03/01.
33. Parker TD, Strachan DD, Welker WI. Technical contribution. Tungsten ball microelectrode for extracellular single-unit recording. Electroencephalogr Clin Neurophysiol. 1973;35(6):647–51. Epub 1973/12/01.
34. Suzuki H, Azuma M. A glass-insulated "Elgiloy" microelectrode for recording unit activity in chronic monkey experiments. Electroencephalogr Clin Neurophysiol. 1976;41(1):93–5. Epub 1976/07/01.
35. Palmer C. A microwire technique for long term recording of single units in the brains of unrestrained animals [proceedings]. J Physiol. 1976;263(1):99P–101. Epub 1976/12/01.
36. Loeb GE, Bak MJ, Salcman M, Schmidt EM. Parylene as a chronically stable, reproducible microelectrode insulator. IEEE Trans Biomed Eng. 1977;24(2):121–8. Epub 1977/03/01.
37. Reece M, O'Keefe JA. The tetrode: a new technique for multi-unit extracellular recording. Soc Neurosci Abstr. 1989;15:1250.
38. Reitboeck HJ. Fiber microelectrodes for electrophysiological recordings. J Neurosci Methods. 1983;8(3):249–62. Epub 1983/07/01.
39. Taylor GF. A method of drawing metallic filaments and a discussion of their properties and uses. Phys Rev. 1923;23(5):655–60.
40. Kaltenbach JA, Gerstein GL. A rapid method for production of sharp tips on preinsulated microwires. J Neurosci Methods. 1986;16(4):283–8. Epub 1986/06/01.
41. Thomas U, Hohl D, Gerber W, inventors. Microprobe system for stereotactic neurotherapy. USA patent US 6799074 B1. 2004.
42. Angle MR, Schaefer AT. Neuronal recordings with solid-conductor intracellular nanoelectrodes (SCINEs). PLoS One. 2012;7(8):e43194. Epub 2012/08/21.
43. Marg E, Adams JE. Indwelling multiple micro-electrodes in the brain. Electroencephalogr Clin Neurophysiol. 1967;23(3):277–80. Epub 1967/09/01.
44. Kubie JL. A driveable bundle of microwires for collecting single-unit data from freely-moving rats. Physiol Behav. 1984;32(1):115–8. Epub 1984/01/01.
45. Barna JS, Arezzo JC, Vaughan Jr HG. A new multielectrode array for the simultaneous recording of field potentials and unit activity. Electroencephalogr Clin Neurophysiol. 1981;52(5):494–6. Epub 1981/11/01.
46. Kruger J, Bach M. Simultaneous recording with 30 microelectrodes in monkey visual cortex. Exp Brain Res. 1981;41(2):191–4. Epub 1981/01/01.
47. Verloop AJ, Holsheimer J. A simple method for the construction of electrode arrays. J Neurosci Methods. 1984;11(3):173–8. Epub 1984/08/01.
48. Jellema T, Weijnen JA. A slim needle-shaped multiwire microelectrode for intracerebral recording. J Neurosci Methods. 1991;40(2–3):203–9. Epub 1991/12/01.
49. Takahashi H, Suzurikawa J, Nakao M, Mase F, Kaga K. Easy-to-prepare assembly array of tungsten microelectrodes. IEEE Trans Biomed Eng. 2005;52(5):952–6. Epub 2005/05/13.
50. Wessberg J, Stambaugh CR, Kralik JD, Beck PD, Laubach M, Chapin JK, et al. Real-time prediction of hand trajectory by ensembles of cortical neurons in primates. Nature. 2000;408(6810):361–5. Epub 2000/12/01.
51. Xu CY, Lemon W, Liu C. Design and fabrication of a high-density metal microelectrode array for neural recording. Sens Actuat A Phys. 2002;96(1):78–85.

52. Gualtierotti T, Alltucker DS. Prolonged recording from single vestibular units in the frog during plane and space flight, its significance and technique. Aerosp Med. 1967;38(5):513–7. Epub 1967/05/01.
53. Gualtierotti T, Bailey P. A neutral buoyancy micro-electrode for prolonged recording from single nerve units. Electroencephalogr Clin Neurophysiol. 1968;25(1):77–81. Epub 1968/07/01.
54. Burns BD, Stean JP, Webb AC. Recording for several days from single cortical neurons in completely unrestrained cats. Electroencephalogr Clin Neurophysiol. 1974;36(3):314–8. Epub 1974/03/01.
55. Salcman M, Bak MJ. A new chronic recording intracortical microelectrode. Med Biol Eng. 1976;14(1):42–50. Epub 1976/01/01.
56. Bradley DC, Troyk PR, Berg JA, Bak M, Cogan S, Erickson R, et al. Visuotopic mapping through a multichannel stimulating implant in primate V1. J Neurophysiol. 2005;93(3):1659–70. Epub 2004/09/03.
57. Musallam S, Bak MJ, Troyk PR, Andersen RA. A floating metal microelectrode array for chronic implantation. J Neurosci Methods. 2007;160(1):122–7. Epub 2006/10/28.
58. Merrill EG, Ainsworth A. Glass-coated platinum-plated tungsten microelectrodes. Med Biol Eng. 1972;10(5):662–72. Epub 1972/09/01.
59. Robinson TF, Hayward BS, Krueger JW, Sonnenblick EH, Wittenberg BA. Isolated heart myocytes: ultrastructural case study technique. J Microsc. 1981;124(Pt 2):135–42. Epub 1981/11/01.
60. Keefer EW, Botterman BR, Romero MI, Rossi AF, Gross GW. Carbon nanotube coating improves neuronal recordings. Nat Nanotechnol. 2008;3(7):434–9.
61. Iijima S. Helical microtubules of graphitic carbon. Nature. 1991;354:56–8.
62. Ferguson JE, Boldt C, Redish AD. Creating low-impedance tetrodes by electroplating with additives. Sens Actuat A Phys. 2009;156(2):388–93.
63. Gao H, Solages C, Lena C. Tetrode recordings in the cerebellar cortex. J Physiol Paris. 2012;106(3–4):128–36. Epub 2011/11/08.
64. Baranauskas G, Maggiolini E, Castagnola E, Ansaldo A, Mazzoni A, Angotzi GN, et al. Carbon nanotube composite coating of neural microelectrodes preferentially improves the multiunit signal-to-noise ratio. J Neural Eng. 2011;8(6):066013. Epub 2011/11/09.
65. Ferguson JE, Boldt C, Puhl JG, Stigen TW, Jackson JC, Crisp KM, et al. Nanowires precisely grown on the ends of microwire electrodes permit the recording of intracellular action potentials within deeper neural structures. Nanomedicine (Lond). 2012;7(6):847–53. Epub 2012/04/06.
66. Westby GW, Wang H. A floating microwire technique for multichannel chronic neural recording and stimulation in the awake freely moving rat. J Neurosci Methods. 1997; 76(2):123–33. Epub 1997/11/14.
67. Blum B, Feldman B. A microdrive for the independent manipulation of four microelectrodes. IEEE Trans Biomed Eng. 1965;12(2):121–2. Epub 1965/04/01.
68. Humphrey DR. A chronically implantable multiple micro-electrode system with independent control of electrode positions. Electroencephalogr Clin Neurophysiol. 1970;29(6):616–20. Epub 1970/12/01.
69. Ainsworth A, O'Keefe J. A lightweight microdrive for the simultaneous recording of several units in the awake, freely moving rat. J Physiol. 1977;269(1):8P–10. Epub 1977/07/01.
70. Ranck JJB. A moveable microelectrode for recording single neurons in unrestrained rats. Iowa City: University of Iowa Press; 1973.
71. Winson J. A compact micro-electrode assembly for recording from the freely-moving rat. Electroencephalogr Clin Neurophysiol. 1973;35(2):215–7. Epub 1973/08/01.
72. Deadwyler SA, Biela J, Rose G, West M, Lynch G. A microdrive for use with glass or metal microelectrodes in recording from freely-moving rats. Electroencephalogr Clin Neurophysiol. 1979;47(6):752–4. Epub 1979/12/01.
73. Bland BH, Sinclair BR, Jorgenson RG, Keen R. A direct-drive, non-rotating version of Ranck's microdrive. Physiol Behav. 1980;24(2):395–7. Epub 1980/02/01.

74. Vertes RP. A device for recording single unit activity in freely-moving rats by a movable fine-wire microelectrode. Electroencephalogr Clin Neurophysiol. 1975;38(1):90–2. Epub 1975/01/01.
75. Knierim JJ, McNaughton BL, Poe GR. Three-dimensional spatial selectivity of hippocampal neurons during space flight. Nat Neurosci. 2000;3(3):209–10. Epub 2000/03/04.
76. Gothard KM, Skaggs WE, Moore KM, McNaughton BL. Binding of hippocampal CA1 neural activity to multiple reference frames in a landmark-based navigation task. J Neurosci. 1996;16(2):823–35. Epub 1996/01/15.
77. Lansink CS, Bakker M, Buster W, Lankelma J, van der Blom R, Westdorp R, et al. A split microdrive for simultaneous multi-electrode recordings from two brain areas in awake small animals. J Neurosci Methods. 2007;162(1–2):129–38. Epub 2007/02/20.
78. Kloosterman F, Davidson TJ, Gomperts SN, Layton SP, Hale G, Nguyen DP, et al. Microdrive array for chronic in vivo recording: drive fabrication. J Vis Exp. 2009. doi:10.3791/1094. Epub 2009/04/22.
79. Korshunov VA, Averkin RG. A method of extracellular recording of neuronal activity in swimming mice. J Neurosci Methods. 2007;165(2):244–50. Epub 2007/08/03.
80. Findlay AL, Horn G, Stechler G. An electrically operated micro-electrode drive for use on unanaesthetized animals. J Physiol. 1969;204(1):4P–6. Epub 1969/09/01.
81. Barmack NH, Hayes DF. A stepper motor controlled microdrive for recording from unanesthetized animals. Physiol Behav. 1970;5(6):705–6. Epub 1970/06/01.
82. Fee MS, Leonardo A. Miniature motorized microdrive and commutator system for chronic neural recording in small animals. J Neurosci Methods. 2001;112(2):83–94. Epub 2001/11/22.
83. Yamamoto J, Wilson MA. Large-scale chronically implantable precision motorized microdrive array for freely behaving animals. J Neurophysiol. 2008;100(4):2430–40. Epub 2008/08/01.
84. Cham JG, Branchaud EA, Nenadic Z, Greger B, Andersen RA, Burdick JW. Semi-chronic motorized microdrive and control algorithm for autonomously isolating and maintaining optimal extracellular action potentials. J Neurophysiol. 2005;93(1):570–9. Epub 2004/07/02.
85. Park S, Yoon E, Lee S, Shin H, Park H, Kim B, et al. The development of a PZT-based microdrive for neural signal recording. Smart Mater Struct. 2008;17:1–7.
86. Yang S, Cho J, Lee S, Park K, Kim J, Huh Y, et al. Feedback controlled piezo-motor microdrive for accurate electrode positioning in chronic single unit recording in behaving mice. J Neurosci Methods. 2011;195(2):117–27. Epub 2010/09/28.
87. Yang S, Lee S, Park K, Jeon H, Huh Y, Cho J, et al. Piezo motor based microdrive for neural signal recording. Conf Proc IEEE Eng Med Biol Soc. 2008;2008:3364–7. Epub 2009/01/24.
88. Ludvig N, Mishra PK, Yan QS, Lasley SM, Burger RL, Jobe PC. The combined EEG-intracerebral microdialysis technique: a new tool for neuropharmacological studies on freely behaving animals. J Neurosci Methods. 1992;43(2–3):129–37. Epub 1992/07/01.
89. Ludvig N, Potter PE, Fox SE. Simultaneous single-cell recording and microdialysis within the same brain site in freely behaving rats: a novel neurobiological method. J Neurosci Methods. 1994;55(1):31–40. Epub 1994/11/01.
90. Ludvig N, Nguyen MC, Botero JM, Tang HM, Scalia F, Scharf BA, et al. Delivering drugs, via microdialysis, into the environment of extracellularly recorded hippocampal neurons in behaving primates. Brain Res Brain Res Protoc. 2000;5(1):75–84. Epub 2000/03/17.
91. van Duuren E, van der Plasse G, van der Blom R, Joosten RN, Mulder AB, Pennartz CM, et al. Pharmacological manipulation of neuronal ensemble activity by reverse microdialysis in freely moving rats: a comparative study of the effects of tetrodotoxin, lidocaine, and muscimol. J Pharmacol Exp Ther. 2007;323(1):61–9. Epub 2007/07/14.
92. Ludvig N, Kovacs L, Kando L, Medveczky G, Tang HM, Eberle LP, et al. The use of a remote-controlled minivalve, carried by freely moving animals on their head, to achieve instant pharmacological effects in intracerebral drug-perfusion studies. Brain Res Brain Res Protoc. 2002;9(1):23–31. Epub 2002/02/20.
93. Fenno L, Yizhar O, Deisseroth K. The development and application of optogenetics. Annu Rev Neurosci. 2011;34:389–412. Epub 2011/06/23.

94. Boyden ES, Zhang F, Bamberg E, Nagel G, Deisseroth K. Millisecond-timescale, genetically targeted optical control of neural activity. Nat Neurosci. 2005;8(9):1263–8. Epub 2005/08/24.
95. Siegle JH, Carlen M, Meletis K, Tsai LH, Moore CI, Ritt J. Chronically implanted hyperdrive for cortical recording and optogenetic control in behaving mice. Conf Proc IEEE Eng Med Biol Soc. 2011;2011:7529–32. Epub 2012/01/19.
96. Tamura K, Ohashi Y, Tsubota T, Takeuchi D, Hirabayashi T, Yaguchi M, et al. A glass-coated tungsten microelectrode enclosing optical fibers for optogenetic exploration in primate deep brain structures. J Neurosci Methods. 2012;211(1):49–57. Epub 2012/09/14.
97. Levick WR. Another tungsten microelectrode. Med Biol Eng. 1972;10(4):510–5. Epub 1972/07/01.
98. Buzsaki G. Large-scale recording of neuronal ensembles. Nat Neurosci. 2004;7(5):446–51. Epub 2004/04/29.
99. Guld C. A glass-covered platinum microelectrode. Med Electron Biol Eng. 1964;2:317–27. Epub 1964/07/01.
100. Sinnamon HM, Woodward DJ. Microdrive and method for single unit recording in the active rat. Physiol Behav. 1977;19(3):451–3. Epub 1977/09/01.
101. Reitbock HJ, Werner G. Multi-electrode recording-system for the study of spatio-temporal activity patterns of neurons in the central nervous-system. Experientia. 1983;39(3):339–41.
102. Chaurasia CS, Muller M, Bashaw ED, Benfeldt E, Bolinder J, Bullock R, et al. AAPS-FDA workshop white paper: microdialysis principles, application and regulatory perspectives. Pharm Res. 2007;24(5):1014–25. Epub 2007/04/27.